WADD TECHNICAL REPORT 60-749
PART I

Wheeton's Library

FACTORS AFFECTING THERMAL SHOCK RESISTANCE
OF POLYPHASE CERAMIC BODIES

AD-A281 579

COPY 1

P. T. B. Shaffer
D. P. H. Hasselman
A. Z. Chaberski

The Carborundum Company
Research and Development Division
Niagara Falls, N. Y.

ICOMPOSITE MAT'LS BRANCH

DTIC QUALITY INSPECTED 2

FEBRUARY 1961

WRIGHT AIR DEVELOPMENT DIVISION

94-18645

94 6 15 1 09

NOTICES

FACTORS AFFECTING THERMAL SHOCK RESISTANCE OF POLYPHASE CERAMIC BODIES

P. T. B. Shaffer

D. P. H. Hasselman

A. Z. Chaberski

The Carborundum Company
Research and Development Division
Niagara Falls, N. Y.

FEBRUARY 1961

WRIGHT AIR DEVELOPMENT DIVISION
AIR RESEARCH AND DEVELOPMENT COMMAND
UNITED STATES AIR FORCE
WRIGHT-PATTERSON AIR FORCE BASE, OHIO

FOREWORD

This report was prepared by The Carborundum Company under USAF Contract No. AF 33 (616)-6806. This contract was initiated under Project No. 7350, "Ceramic and Cermet Materials," Task No. 73500, "Ceramic and Cermet Materials Development." The work was administered under the direction of the Materials Central, Directorate of Advanced Systems Technology, Wright Air Development Division, with Capt. Ray H. Wilson and Mr. K. S. Mazdiyasni acting as project engineers.

This report covers work conducted from October 1959 to October 1960. The research will be continued for an additional year.

The research has been conducted by the Applied Research Branch, Research and Development Division, of The Carborundum Company under the general supervision of Dr. W. A. Lambertson and the direct supervision of Mr. C. E. Shulze.

ABSTRACT

An investigation of the factors which effect the thermal shock resistance of polyphase ceramic systems has been conducted using the model system zirconium carbide-graphite. The research has been divided into two areas:

1. Theoretical calculations of the individual material properties, which show that the included graphite particles may be regarded as spherical pores.

2. Experimental data, which substantiate the postulate that increased thermal shock resistance is a result of an increase in the ratio of strength over Young's modulus, brought about by the addition of the low Young's modulus phase.

PUBLICATION REVIEW

This report has been reviewed and is approved.

FOR THE COMMANDER:

W. G. Ramke
Chief, Ceramics and Graphite Branch
Metals and Ceramics Laboratory
Materials Central

TABLE OF CONTENTS

PAGE

TABLE OF CONTENTS
(Continued)

PAGE

LIST OF FIGURES

LIST OF FIGURES
(Continued)

LIST OF TABLES

I. INTRODUCTION

The rapidly increasing demand for materials suitable for use in the aircraft and missile industries has placed severe limitations on the high temperature applications of metals and metal alloys. Ceramic materials although possessing excellent high temperature properties are limited because of poor thermal shock resistance.

Recently, ceramic materials were developed based on a high Young's modulus continuous phase and a low Young's modulus dispersed phase with markedly improved thermal shock resistance.[1] Simultaneously the high temperature properties of the high Young's modulus phase such as strength and erosion resistance, were retained.

The purpose of this research project was to determine the fundamental reasons for the improved thermal shock resistance of these material and to extend the concept of high Young's modulus continuous phase-low Young's modulus dispersed phase ceramic materials to new classes of refractory material systems.

II. FUNDAMENTAL CONSIDERATIONS

The thermal shock resistance of a ceramic material is defined as its ability to withstand sudden temperature changes without fracturing.

The factors which will affect the performance of a ceramic material undergoing thermal shock can be listed in three groups as follows:

(i) Factors defining the actual thermal shock conditions such as the temperature difference to which the ceramic body is subjected and the heat transfer coefficient which is a measure of the severity of the thermal shock.

(ii) Factors determining the geometry of the ceramic body such as its size and shape.

(iii) Factors determining the material properties of the ceramic body. These material factors consist of Young's modulus, strength, Poisson's ratio and the properties describing the thermal behavior of the ceramic such as its linear expansion coefficient, thermal conductivity, and diffusivity.

Of these three groups the first two determine the conditions and severity of the thermal shock. The factors of the third group determine the magnitude of the thermal stresses that will arise due to the thermal shock and the ability of the ceramic body to withstand these stresses.

These material factors can be combined in so-called thermal stress resistance factors defined by:

$$R = \frac{S_t (1 - \nu)}{\alpha E}$$

$$R' = \frac{S_t (1 - \nu)k}{\alpha E}$$

$$R'' = \frac{S_t (1 - \nu)a}{\alpha E}$$

where R, R' and R" are the thermal stress resistance factors, their choice depending on the actual condition of thermal shock. The symbol S_t stands for the strength of the ceramic material. As ceramic materials subjected to thermal shock generally fail in tension rather than in shear or compression, the tensile strength is generally used as the criterion for failure rather than the compressive or shear strength. The symbols ν, α and E stand for Poisson's ratio, the coefficient of thermal expansion and Young's modulus respectively. The factors k and a denote the thermal conductivity and diffusivity.

As the thermal shock resistance of a ceramic material is governed mainly by its mechanical and thermal properties, as indicated above, an improvement of the thermal shock resistance of the high Young's modulus continuous phase-low Young's modulus dispersed phase composite material (hereafter referred to as the high E - low E material) is, therefore, due to a change in one or more of the material properties such that these changes lead to an increase in the thermal stress resistance factors.

Since all of the material properties which enter into the thermal shock resistance factor react simultaneously during exposure of a body to thermal stress, it will not be possible to isolate and determine which

single property contributes to the improvement of thermal shock resistance. Therefore, in order to investigate the fundamental reason for the improved thermal shock, each material property will have to be determined individually. This can be done by calculating the mechanical and thermal properties on the basis of suitable models or by determining the individual material properties experimentally.

The approach taken in this investigation was to calculate the mechanical and thermal properties on the basis of suitable mechanical models. These calculations were then compared with the actual values obtained experimentally. Thermal shock tests will then be performed to correlate the individual data with the actual overall thermal shock resistance.

The model ceramic system selected for this study was the mixture zirconium carbide-graphite. Zirconium carbide has a Young's modulus approximately equal to 50×10^6 pounds per square inch, while Young's modulus of graphite is approximately equal to 1.0×10^6 pounds per square inch. The ratio of the Young's moduli is, therefore, approximately 0.02.

III. THEORETICAL CONSIDERATIONS

A literature survey of the thermal shock behavior of ceramic materials revealed little or no thermal shock resistance data for heterogeneous systems as a function of the relative material properties of the individual components.

Numerous calculations could be found of thermal stresses both in the steady and transient state for homogeneous materials with given mechanical and thermal properties.

These calculations, however, give the stresses developed, without taking into account the strength of the material. Without knowledge of the material properties such as strength and Young's modulus, the rigorous calculation of stresses within a body are of little value in determining whether a material will survive a thermal shock of given severity.

Considerable work was done, however, to determine the individual material properties of heterogeneous systems as a function of volume fraction and material properties of the individual components. The

calculations are based on the assumption that no reaction occurred between the components during manufacture and that the heterogeneous body can be regarded as a mixture of the individual components. One of the major difficulties in calculating the overall mechanical and thermal properties of heterogeneous systems is the selection of a suitable model or models on which these calculations can be based. The choice of this model will be governed by the individual properties of each component, the way each component is distributed through the body, and the volume fraction and particle size or shape of each component. Also for the calculation of a particular material property one mechanical model will lend itself more readily than others.

Various models employed in previous investigations of the properties of heterogeneous systems are to be found in the literature. One model used in the calculation of the coefficient of thermal expansion and of the thermal conductivity consists of a structure composed of parallel alternate slabs of the two components. By changing the relative orientation of the slabs to the applied stress or direction of heat flow this model lends itself very well to establishing the boundary values of the material property under consideration. Regardless of the microstructure of the heterogeneous system the actual values of the material properties will fall between these boundary values.

Another model widely used, especially in the calculation of such material properties as the moduli of elasticity and internal stresses, consists of a single spherical or elliptical particle imbedded in an infinite matrix. This model most closely represents the actual microstructure of the high E - low E material. The high Young's modulus phase is represented by the infinite matrix, whereas the low Young's modulus material is represented by the single particle contained within this matrix.

The material properties which can be calculated most readily on the basis of these two models are the coefficient of thermal expansion, the modulus of elasticity and the thermal conductivity. In addition, these models lend themselves to predicting the strength behavior of these heterogeneous systems.

The initial approach then towards the solution of the problem of the improved thermal shock resistance of the high E - low E materials was to calculate the overall material properties of the heterogeneous system as a function of the material properties and volume fraction of the individual components.

A. Coefficient of Thermal Expansion

The coefficient of thermal expansion of heterogeneous systems was determined by many investigators including Kingery[2] and Coble[3]. Kingery noted that for the systems W-MgO and Al-SiO$_2$ the thermal expansion data are not simply averages of the values of the individual components but agree quantitatively with calculations based on the assumption that substantial residual microstresses result from the mutual restraints of each phase on cooling. Coble gives the following equation for the coefficient of thermal expansion, which agrees very well with expansion data obtained experimentally,

$$\alpha_{het.} = \alpha_2 - \frac{(\alpha_2 - \alpha_1)\dfrac{E_1 F_1}{1 - \nu_1}}{\dfrac{E_1 F_1}{1 - \nu_1} + \dfrac{E_2 F_2}{1 - \nu_2}} \qquad (1)$$

where $\alpha_{het.}$ is the coefficient of thermal expansion of the heterogeneous system:the subscripts 1 and 2 refer to component 1 and 2 respectively. E is Young's modulus, α is the coefficient of thermal expansion, ν is Poisson's ratio, and F is the volume fraction. This equation is based on the mechanical model composed of parallel slabs with the expansion taking place in the plane of the slabs, and will give the coefficient of expansion of the high E - low E material for all compositions as long as the material with the high elastic modulus is the continuous phase.

Assuming $\nu_1 = \nu_2$, and defining $k = E_2/E_1$, the ratio of the Young's moduli, where the subscript 1 now refers to the high Young's modulus continuous phase and the subscript 2 to the low Young's modulus dispersed phase, equation (1) can be simplified to read:

$$\alpha_{het.} = \alpha_2 - \frac{(\alpha_2 - \alpha_1) E_1 F_1}{E_1 F_1 + KE_1 F_2} \qquad (2)$$

Inspection of this equation reveals that the coefficient of thermal expansion of the heterogeneous system depends on the coefficients of thermal expansion of the components, the ratio of the Young's moduli of the components, and their volume fractions. In the system

under study k, is approximately equal to 0.02. Substitution of this value for k, into equation (2) shows that the overall coefficient of thermal expansion of this heterogeneous system is approximately equal to the coefficient of expansion of the high Young's modulus component even at high volume fraction of the low Young's modulus phase. Only when the volume fraction of the high elastic modulus phase approaches zero will the calculated value of the overall coefficient of expansion approach the value of the coefficient of thermal expansion of the dispersed low elastic modulus phase.

The foregoing discussion, therefore, indicates that for the heterogeneous system under study with volume fractions of the low Young's modulus component of less than 0.5 or 0.6, the overall coefficient of thermal expansion is for all practical purposes equal to the coefficient of thermal expansion of the high elastic modulus component. From the point of view of thermal shock resistance, this independence of the coefficient of thermal expansion with respect to the volume content of low Young's modulus component cannot explain the higher thermal shock resistance of the high E - low E composite material. For the measured values of the coefficient of thermal expansion see Experimental Results.

B. Young's Modulus

A literature survey revealed that several attempts were made to calculate the elastic constants of heterogeneous systems as a function of the Young's moduli and volume fraction of the individual components.

Paul[4] attacked the problem with a "strength of materials" approach. A careful analysis of his calculations and the assumptions on which these were based revealed that his equation can be useful to predict the elastic constants of heterogeneous systems composed of materials with elastic constants which differ by no more than a factor of two or three. However, for a heterogeneous system such as the high E - low E material with a ratio of Young's moduli of approximately fifty, Paul's equations are no longer valid and his predicted values are considerably in error especially at high volume fractions of the low E - component.

An exact solution was given by Jane M. Dewey[5], who calculated the elastic constants of a material containing small volume fractions of

spherical particles. MacKenzie[6] gives equations for the elastic
constants of materials containing spherical holes,which is a special
case of the equations given by Jane M. Dewey. MacKenzie's equa-
tions, however, are valid for greater volume fractions of spherical
holes than Jane M. Dewey's equations. In the investigation of the
high E - low E material, Dewey's equations are of particular interest
as they lend themselves well to the calculation of relative differences
between the overall elastic constants of a material containing spheri-
cal particles of graphite and the same material containing the same
volume fraction of spherical holes. By substitution of the respective
values into the equation for the effective shear modulus, it can be
shown (Appendix A) that for small volume fractions of low - E
material where k is much less than one that to a first approximation
the following relation holds.

$$\frac{\text{shear modulus of composite with low E material}}{\text{shear modulus of composite with spherical pores}} = 1 - 4\,k\,\phi$$

where k is the ratio of shear moduli of the components and ϕ is the
volume fraction of the low Young's modulus phase. For the system
under study k is approximately equal to 0.02. Therefore at a volume
fraction of graphite of 0.1 the relative difference between shear moduli
is 0.8 percent. It can, therefore, be concluded that from the point of
view of shear modulus, the low E material can be regarded for all
practical purposes as being equivalent to pores of the same shape and
concentration.

For the system under study, therefore, the elastic constants can
be predicted from MacKenzie's equations rather than from Dewey's
equation. Not only is the introduced error smaller but also MacKenzie's
equations are valid for greater volume fractions on the dispersed phase.

The equation for the effective shear modulus as calculated by
MacKenzie is given by:

$$\frac{u_0 - u}{u_0} = \frac{5\,(1-\rho)\,(3k_0 + 4\,u_0)}{(9\,k_0 + 8\,u_0)} + 0\,(1-\rho)^2$$

where the subscript refers to the nonporous material. K is the bulk
modulus, u is the shear modulus, ρ is the density of the porous
material relative to the nonporous material. (See Reference 3)

The term $\dfrac{5\,(3\,k_0 + 4\,u_0)}{(9\,k_0 + 8\,u_0)}$ gives the slope of the relative shear modulus against porosity curve at zero porosity. The additional term $O\,(1 - \rho)^2$ is a successive parabolic approximation. On this basis O can be evaluated by setting $u = o$ and $\rho \approx o$.

The actual value of the term $\dfrac{5\,(3\,k_0 + 4\,u_0)}{(9\,k_0 + 8\,u_0)}$ depends on Poisson's ratio but is usually approximately equal to 2.

Although this equation gives the effective shear modulus, it also predicts correctly the behavior of Young's modulus as verified experimentally by Coble[3].

The calculated Young's modulus curve versus porosity is presented graphically in Figure 9.

C.   Strength

The material factors discussed so far are those which determine the magnitude of the thermal stresses which will occur for a given temperature distribution.

The ability, however, of the ceramic body to withstand these thermal stresses is dictated by its strength. Since ceramic materials usually fail in tension, as do most other brittle materials, the magnitude of the tensile strength determines whether a ceramic body will survive a thermal shock of given severity.

Many attempts have been made to calculate the strength of materials. However, the calculated values usually differ from the measured values by orders of magnitude. This discrepancy is attributed to the presence of flaws within the material, which seriously affect the overall strength of the body. Therefore, the strength used in engineering computations must be determined experimentally.

In order to estimate the tensile strength of a heterogeneous system such as the high E - low E material on a basis of the strength of the individual components, use can be made of the strengths of the components determined experimentally.

Some of the factors to be considered in this estimation of strength are:

1. The strength of each component

2. The strain at fracture of each component

3. The microstructure of the heterogeneous system such that a suitable mechanical model may be selected

4. The distribution of stress through the high E - low E material, with special regard to stress concentrations which may affect strength.

In addition to these factors an estimation should be made of the internal stresses which arise on cooling due to differences in thermal expansions of the individual components. In the case of heterogeneous systems the presence of internal stresses may lower or increase the strength at room temperature. If the material with the lowest strain at fracture is under compression, strength may be increased substantially. If, however, the same material is under tension the tensile strength may be reduced to a value to make the composite material practically useless.

In order to select a suitable mechanical model, computations were made to establish the role of the low E component in the high E - low E material from the point of view of its effect on the stress distribution through the high E material.

Considerable work was done by other investigators[7,8,9] to calculate the stress-concentration factors around particles of various shape contained in an infinite medium with elastic constants different from the elastic constants of the included particle. Analysis of equations for the stress concentration factors around spherical inclusions calculated by Goodier[7] showed that for all practical purposes the lowE material within the continuous high E material can be considered as being equivalent as spherical porosity. A similar conclusion was reached for the overall elastic constants, as discussed previously.

It can be shown that the following ratio approximately holds:

$$\frac{\text{stress concentrations around spherical particle}}{\text{stress concentrations around spherical pore}} = 1\text{-}2\ K$$

where K is the ratio of the shear moduli of the particle and the surround-

ing matrix, and is very much less than one.

For the system under study with K = 0.02 the stresses in the high E material around a spherical low E particle, therefore, differ by a factor approximately equal to 0.96.

As the low E dispersed particles are approximately equidimensional, the model which most closely represents the actual material would be a body composed of the high E material containing the same volume fraction of spherical holes. From the point of view of strength, a model composed of alternate slabs of the high E material and open spaces with the stress applied parallel to the slabs would be most convenient as the reduction in strength will be proportional to the decrease in cross-sectional area. This assumption also holds for a material containing spherical holes if fracture takes place along a cross-sectional plane. However, in the case of spherical holes, fracture is more likely to occur along the maximum diameter of the holes. Therefore, the decrease in strength is governed by the decrease in effective cross-sectional area determined by the projected cross-sectional area of the spherical holes intercepted by a unit plane. Using the equations of Fullman[15] it can be shown that the projected cross-sectional area of spherical holes intercepted by a unit plane is given by 1.5ϕ where ϕ is the volume fraction of the holes.

The actual fracture mechanism will fall between these two limiting cases. The strength of the high E - low E material may then be given by:

$$ S = S_o (1 - K \phi) $$

where S is the strength of the high E - low E component, and S_o is the strength of the high E component without additions of the low E particles, K is a constant given by $1.0 < K < 1.5$, and ϕ is the volume fraction of the low E component.

In the equation for the strength of the high E - low E material as given above the presence of any internal stresses was neglected. As discussed previously these internal stresses may affect strength appreciably. Various attempts have been made to calculate internal

stresses on the basis of suitable mechanical models. Exact solutions for the stresses in a particle embedded in an infinite matrix were given by Robinson[11] and Edwards[12]. To calculate the stresses in a heterogeneous system Gurland[13] used the model of a single spherical inclusion embedded in an infinite mass, the latter taking on the properties of the alloy instead of those of the matrix phase.

The radial stresses σ_{r_1} inside the spherical particle as calculated by Gurland is given by

$$\sigma_{r_1} = \frac{2 E_1 E_2 (\alpha_2 - \alpha_1) \Delta T}{(1 + \nu_2) E_1 + 2(1 - 2 \nu_1) E_2}$$

where the subscript 1 refers to the embedded particle and the subscript 2 refers to the continuous phase.

E is Young's modulus

ν is Poisson's ratio

α is the coefficient of thermal expansion

and ΔT is the temperature difference through which the composite is cooled. Writing $E_1/E_2 = K$, the ratio of the respective Young's moduli, and rearranging gives for σ_{r_1}:

$$\sigma_{r_1} = \frac{2E_1 (\alpha_2 - \alpha_1) \Delta T}{(1 + \nu_2) K + 2 (1 - 2\nu_1)}$$

for $K << 1$ this becomes

$$\sigma_{r_1} = \frac{E_1 (\alpha_2 - \alpha_1) \Delta T}{(1 - 2 \nu_1)}$$

Substitution of typical values such as:

$E = 1.0 \times 10^6$ pounds per square inch $(\alpha_2 - \alpha_1) = 5 \times 10^{-6}/{}^{\circ}C.,$
$\Delta T = 1.5 \times 10^{3\,\circ}C.$ $\nu = 0.25$

yields a value of 15,000 pounds per square inch for the stresses in the embedded particle. These stresses in the matrix will be compressive

if the coefficient of expansion of the embedded particle is smaller than the coefficient of expansion of the matrix and tensile if greater.

In order to evaluate the average stress in the surrounding medium it becomes necessary to decide on the effective range of influence of the embedded particle. An expression developed by Gurland[14] is based on the mean-free path. For spheres of uniform size, the mean-free path P between particles as given by Fullman: [15] $P = \frac{4}{3} \rho \frac{(1 - \phi)}{(\phi)}$

where ρ is the radius of the embedded particles and ϕ the volume fraction. The radius of influence R of the particle measured from its center is approximated by $R = \rho + 1/2 P$ or by the ratio $k = R/\rho = 1 + \frac{2}{3} \frac{(1 - \phi)}{\phi}$. The average radial and tangential stresses in the medium denoted by σ_{r2} and σ_{c2} respectively are then given by

$$\sigma_{r2} = \frac{3 \sigma_{r1} \ln k}{k^3 - 1}$$

and

$$\sigma_{c2} = \frac{3}{2} \frac{\sigma_{r1} \ln k}{k^3 - 1}$$

where σ_{r1} is the radial stress in the embedded particle. Assuming a volume fraction of embedded particles with low Young's modulus of 0.25, and substitution of the radial stress in the particle as calculated above gives for the mean values of the radial and tangential stress in the medium 1,900 and -950 pounds per square inch respectively. It may be noticed that the radial stresses are of the same sign and the tangential stresses of opposite sign to the radial stresses.

In the systems under study the low Young's modulus component usually has the lower coefficient of thermal expansion and is, therefore, under compression at room temperature. The tangential stresses in the medium are, therefore, tensile and will be the stresses affecting the strength of the composite. Comparison of the calculated tangential stress in the medium with the usual tensile strength of a ceramic material of approximately 20,000 pounds per square inch or higher shows that the internal stresses are expected to affect strength only slightly and may lower it by a few percent.

Substitution of a value for Young's modulus into the equation for the internal stresses in the particle comparable to Young's modulus of the medium shows that the internal stresses in the high E - low E material are lower by several orders of magnitude than the internal stresses in a heterogeneous system composed of two high E components, which supports the previous conclusion that the low E dispersed phase can be regarded as porosity.

For the actual values for the strength of the high E - low E material see the section Experimental Results.

D. Thermal Conductivity and Thermal Diffusivity

The factors discussed thus far determine the actual thermal shock resistance of a ceramic for a given temperature distribution within the ceramic body. This temperature distribution as a function of time and position is governed by the thermal conductivity and thermal diffusivity.

In the system under study, additions of the low E dispersed phase to the high E continuous phase will, in addition to changing the mechanical properties, also affect the thermal conductivity and diffusivity.

Various attempts have been made to calculate the thermal conductivities of heterogeneous systems[16, 17]. The various relations depend on the actual distribution of the individual components. An expression developed by Eucken[17] describes most accurately the system under study and gives the overall thermal conductivity of a continuous phase with spherical inclusions and is given by:

$$k_m = k_1 \frac{1 + 2\phi_1 \frac{(1 - k_1/k_2)}{(2k_1/k_2 + 1)}}{1 - \phi_1 \frac{(1 - k_1/k_2)}{(2k_1/k_2 + 1)}}$$

where k_m is the conductivity of the mixture. k_1 and k_2 are the conductivities of the continuous and dispersed phases respectively and ϕ_1 is the volume fraction of the continuous phase.

The thermal diffusivity, a, of a material is defined by

$$a = \frac{K}{c\,\rho}$$

where K is the thermal conductivity, c the specific heat, and ρ the density.

The change in thermal diffusivity, therefore, is governed by the simultaneous changes in thermal conductivity, specific heat and density. The changes in specific heat and density will be a linear function between the values of the components according to

$$c = \phi_1 c_1 + \phi_2 c_2$$

and

$$= \phi_1 \rho_1 + \phi_2 \rho_2$$

where the subscripts refer to the components and the symbols as defined above.

The thermal diffusivity can then be expressed as follows:

$$a_m = \frac{K_m}{(\rho_1 \phi_1 + \rho_2 \phi_2)(c_1 \phi_1 + c_2 \phi_2)}$$

where K_m is the thermal conductivity as given by Eucken's equation.

E.   Thermal Shock Resistance

Discussed so far were the individual material properties which enter the thermal shock resistance of the high E - low E material. The relative importance of these individual properties may be discussed by means of the equation developed by Crandall and Ging[18] which gives the maximum temperature difference to which a ceramic body of simple geometric shape can be subjected without fracturing. This is given by:

$$\Delta T = A \left(\frac{S_t (1-\nu)}{\alpha E} \right) \left(1 + \frac{2}{\beta} \right)$$

where ΔT is the maximum difference between the two ambient temperatures between which the ceramic body can be transferred without fracturing. A is a constant which depends on the shape of the

ceramic body and is equal to 2.5 for a sphere, 2 for a cylinder and 1.5 for a flat plate.

ν is Poisson's ratio

S_t is the tensile strength

α is the coefficient of expansion

E   is Young's modulus

β is Biot's modulus defined by $\beta = \dfrac{ah}{K}$

where a is the radius of the ceramic body in the case of a sphere or cylinder, or half the thickness in the case of a flat plate; h is the surface heat transfer coefficient and K the thermal conductivity.

It may be noted that this equation is the sum of two terms. The first term gives the maximum temperature difference within the ceramic body which can be supported without fracture. The second term gives the additional temperature difference to which the body can be subjected during the period of heat transfer without having the internal temperature difference exceed the temperature difference as given by the first term. This first term is dictated by the material properties only, whereas the second term depends on the type of thermal shock, i.e. magnitude of h, and the size of the body. Examination of the second term shows that the thermal conductivity of a material is only of secondary importance, and an increase in thermal conductivity will not necessarily lead to an increase in thermal shock resistance. Only for a given heat transfer coefficient and body size such that Biot's modulus is small enough that the term $2/\beta$ is comparable to unity will an increase in thermal conductivity increase the thermal shock resistance. The answer to the improved thermal shock resistance of the high E ~ low E material is, therefore, not to be found in a possible change in thermal conductivity but in a change in the term $\dfrac{S_t\ (1-\nu)}{\alpha E}$.

As discussed previously, the coefficient of thermal expansion of the high E - low E materials will be essentially constant for the range of volume fractions of low E component for which the high E component remains continuous. The term $1 - \mathcal{V}$ is not expected to change appreciably. The improvement of the thermal shock resistance of the high E - low E material can, therefore, only be due to an increase in the ratio of strength to Young's modulus.

On the basis of spherical porosity the ratio of strength to Young's modulus for small volume fractions of the low E component can to a first approximation be given by

$$\frac{S}{E} = \frac{S_o}{E_o} \frac{(1-K\phi)}{(1-2\phi)} \qquad \text{where } 1.0 < K < 1.5.$$

This relation indicates that, regardless of the value of K, additions of spherical particles of the low E component results in an increase in the ratio of strength over Young's modulus. This in turn increases the thermal shock resistance.

It may be noted that the temperature difference to which a ceramic body may be subjected is independent of the thermal diffusivity. For a given thermal conductivity a difference in thermal diffusivity only affects the time at which a given temperature or stress distribution occurs within the specimen.

IV. EXPERIMENTAL

The experimental part of this investigation consisted of measuring the physical properties of several zirconium carbide-graphite composites, this system being selected as the high E - low E model ceramic system. The properties measured were the coefficient of thermal expansion, Young's modulus together with Poisson's ratio, and modulus of rupture. In addition, some thermal shock tests and experiments to measure internal stresses were also performed.

A. Materials

The materials selected for this study were zirconium carbide and graphite. The zirconium carbide was produced by the New Products Branch of The Carborundum Company and was in the form of -325 mesh powder. The spectrographic analysis was as follows:

> 0.1   - 0.5 percent Fe,
> 0.01   - 0.05 percent Cr, Ca,
> 0.005 - 0.01 percent B, Si, Ti

The graphite used was manufactured by the International Graphite and Electrode Company. This graphite was ground and screened to a particle size between 70 mesh and 100 mesh. Microscopic examination showed the individual graphite particles to be approximately equidimensional.

B. Preparation of Test Specimens

Mixtures of zirconium carbide and graphite of various compositions ranging from 0 to 55 volume percent graphite were intimately mixed in a rotary mill. Bodies measuring 4-1/2 inches in diameter by 4 inches high were then hot pressed in graphite molds at a temperature of 2250°C. and pressure of 2000 pounds per square inch. Test specimens of suitable size for the determination of the various properties were then diamond-sawed from these hot-pressed bodies and subsequently ground.

For the thermal shock test, spheres of one and two inch diameter containing similar volume fractions of graphite as in the hot-pressed pieces described above were hot pressed in suitable graphite molds. After hot pressing, the spheres were ground to a roundness of better than 0.01 inches.

In order to determine the degree of dispersion of the graphite particles within the zirconium carbide phase, polished sections were prepared of test specimens and spheres containing various volume fractions of graphite. Microscopic investigation of the polished sections revealed that the graphite particles were evenly distributed throughout the zirconium carbide. Photomicrographs of various compositions are shown in Figure 1.

C. Equipment

1. Coefficient of Thermal Expansion

Figure 2 shows the apparatus to measure the coefficient of thermal expansion. It consists of a dense, impervious, closed-end silicon carbide tube attached to a water-cooled brass flange. A silicon carbide rod extends from the sample, located in the bottom of the tube, to an Ames micrometer dial which measures the differential expansion between the sample and the silicon carbide tube. The assembly is covered by a glass bell jar which permits atmosphere control within the tube. The dilatometer may be heated in any vertical furnace of suitable size and is currently located within an inductively heated graphite susceptor. Temperatures were measured with an optical pyrometer sighted on the lower end of the silicon carbide tube. Provisions were also made for use of thermocouples located adjacent to the sample when measurements at lower temperatures are desired.

The dilatometer was calibrated to $1350^\circ C$. by means of a standard sample in the form of a single crystal of aluminum oxide obtained from the Linde Company. At higher temperatures the equipment was calibrated by means of a rod of spectroscopic grade graphite, obtained from the National Carbon Company, whose expansion was found to be linear above $1000^\circ C$. This enabled the calibration curve to be extrapolated to $2000^\circ C$. The experimental accuracy has been estimated to be better than two percent.

2. Young's Modulus, Shear Modulus, and Poisson's Ratio

The sonic method was selected to determine Young's modulus of the zirconium carbide - graphite composites. The method consists of determining the frequency of the first mode of flexural vibration of a specimen of suitable geometry. By means of equation given by Pickett[19], Young's modulus was then calculated. By vibrating the test specimens in the torsional mode the shear modulus was determined. Poisson's ratio was then calculated by means of the relationship between Young's modulus and the shear modulus given by:

$$\mathcal{U} = \frac{E}{2G} - 1$$

where ν is Poisson's ratio and E and G, Young's modulus and the shear modulus respectively.

The specimens selected consisted of rectangular bars measuring approximately three by one half by one quarter inches.

For measurements at room temperature the bars were suspended between elastic bands located at the nodes so as not to interfere with the vibrations. The bars were driven by a cutting head driver of type A41-8 manufactured by the Astatic Corporation. The vibrations were detected by means of a microphone held directly above the specimen. The correct mode of vibration was detected by sprinkling the vibrating bars with fine silicon carbide powder. From the nodal pattern in which the silicon carbide powder arranged itself the proper mode of vibration could be determined.

To measure the dependence of Young's modulus on temperature a Globar®-heated furnace, shown diagrammatically in Figure 3, will be employed. The test specimens are to be placed in a graphite specimen holder (Figure 4) which allows accurate positioning of test specimens within the furnace. Within the graphite boat the specimen is supported by graphite pins located at the nodes.

The specimens will be driven by means of a metal or graphite rod attached to a speaker located outside the furnace. The vibrations are to be detected by means of another rod connected to a crystal contact microphone also located outside the furnace and supported by a spring to reduce the load on the specimen. The temperature within the furnace will be measured by means of a thermo-couple and at higher temperatures by means of an optical pyrometer.

3. Modulus of Rupture

The strength of the zirconium carbide-graphite composites was determined by means of modulus of rupture measurements. Specimen size was approximately three by one half by one quarter inches. At room temperature the specimens were subjected to three point loading on a Riehle testing machine with a span of two and one half inches at a strain rate of 0.05 inches per minute. The modulus

of rupture for a particular graphite content was determined by averaging the modulus of rupture values obtained from eight to ten separate experiments. The apparatus to determine modulus of rupture values at temperatures to 2400°C. is shown in Figure 5. It consists of two pieces of graphite which fit together along eight bearing surfaces in order to insure correct alignment. The lower piece supports two graphite pins in oversize holes as does the upper anvil. The test bar placed within the apparatus is therefore subjected to four point loading. This graphite assembly is located inside a heavy wall graphite crucible which is heated inductively, Figure 6. In order to compare the modulus of rupture values determined at room temperature under three point loading with those obtained under four point loading, a number of test bars were broken at room temperature in the graphite assembly described above. The resulting values were nearly identical to those obtained under three point loading.

4. Thermal Conductivity

The apparatus to measure thermal conductivity is a copy of that devised by Francl and Kingery[20] at M.I.T. and in use at Alfred University, Figure 7. It is capable of precise measurements up to 1200°C. It consists of a heater and a heat sink arrangement between which are stacked three samples; two standards with the unknown in between. A temperature gradient is established and an equivalent gradient is then adjusted in the surrounding ceramic muffle by means of five separate, independent heaters. This minimizes the lateral heat flow between the samples and the protective muffle. The conductivity is determined by the inverse ratio of the thermal gradients within the three samples. The standard materials consisted of Wesgo alumina,produced by the Western Gold and Platinum Company, Belmont, California; nickel; and cold-rolled Inconel,obtained from the International Nickel Company.

D. Thermal Shock Testing

The method selected to measure the actual thermal shock resistance of the zirconium carbide-graphite system consisted of subjecting hot-pressed bodies of these materials to a radiation convection boundary condition. The sphere was selected as the most convenient body shape. Solutions for the thermal shock analysis of spherical shapes were given by Crandall and Ging[18], who showed that the method of thermally shocking a spherical body

lends itself well to correlating the individual material property values with the overall thermal shock resistance.

In addition to subjecting the spheres to thermal shock by sudden heating, quenching experiments were also performed. These consisted of heating the spheres slowly to the desired temperatures and suddenly quenching in water at room temperature.

The furnace employed for the thermal shock tests consisted of a Pereny three inch diameter graphite-tube furnace provided with argon atmosphere control.

To subject the spheres to thermal shock by heating, the furnace was brought up to the desired temperature. A sphere was then placed on a small graphite assembly which insured uniform heating boundary conditions, and pushed into the tube furnace. The sphere was continuously observed to determine the mode of fracture.

To determine the temperature difference which will cause a sphere to fracture the furnace temperature was raised in steps of $100^{\circ}C.$, and a number of spheres were subjected to thermal shock at each temperature.

For the quenching experiments the spheres were slowly pushed into the same tube furnace and, when thermal equilibrium was reached, pushed out of the furnace and rolled into a container with water at room temperature.

The temperature difference which would fracture a sphere by quenching was determined by continuously raising the temperature of the furnace, thereby increasing the temperature difference of quenching.

E. Experimental Results

1. Coefficient of Thermal Expansion

The results obtained for the coefficient of expansion of the zirconium carbide-graphite composites are given in Table I. It may be noted that the coefficient of expansion does not change with graphite content, any variation being entirely within the range of experimental error.

2. Young's Modulus, Shear Modulus, Poisson's Ratio

Table No. II shows the results obtained for Young's modulus, shear modulus and Poisson's ratio at room temperature. The test specimens were cut perpendicularly to the hot-pressing direction. The values represent the mean of at least ten individual measurements. The maximum deviation was no more than two percent. The porosities were calculated from the overall density of the composite body and the densities and volume fractions of the components, assuming theoretical densities of 6.70 grams per cubic centimeter and 1.70 grams per cubic centimeter for zirconium carbide and graphite.

Included also are the elastic constants of graphite perpendicular and parallel to the extrusion direction. Poisson's ratio for graphite was not calculated, as the relationship between Young's modulus, shear modulus and Poisson's ratio is valid for isotropic materials only. Initial measurements on small graphite bars approximately three by one-half by one-quarter inches showed a large surface effect. Removal of a layer seven thousandths of an inch thick from the surface changed the value of Young's modulus in one instance from 1.107×10^6 pounds per square inch to 1.338×10^6 pounds per square inch. It is thought that this may be due to the presence of small surface cracks. The values for graphite in Table No. II were obtained on large bars measuring approximately five by one by one inches, to minimize surface effects. Figure 8 shows Young's modulus plotted against volume fraction graphite. As the graphite can be regarded as additional porosity, as discussed in the section on strength, Young's modulus was plotted against volume fraction graphite plus porosity as shown in Figure 9. The dotted line represents MacKenzie's[6] equation for spherical porosity. It may be noted that agreement is excellent.

Experiments were conducted to determine any orientation dependence of the elastic constants with respect to the direction of hot pressing. The elastic constants of a number of bars cut parallel to the hot-pressing direction were compared with those elastic constants of bars cut perpendicular to the hot-pressing direction. No difference was found to exist.

3. Strength

The results for the modulus of rupture of the zirconium carbide-graphite bodies as a function of graphite content and temperature are tabulated in Table III and shown graphically in Figures 10 to 17. A plot of modulus of rupture as a function of volume fraction graphite plus porosity is also included. It may be noted that the modulus of rupture at room temperature decreases with increasing graphite content, but that the modulus of rupture at higher temperatures seems to be independent of graphite content. In other words, the modulus of rupture becomes less dependent on temperature with higher graphite content. In addition, it may be noticed that an apparent maximum exists at approximately 1000°C. in the modulus of rupture against temperature curves. In order to determine whether this was due to the presence of internal stresses, test bars of various compositions were annealed at 1500°C. for two hours. Young's modulus was then determined at room temperature and modulus of rupture at room temperature and at 1000°C. No change in either of these two properties was found.

4. Ratio of Strength over Young's Modulus

As discussed under "Thermal Shock Resistance", the ratio of strength over Young's modulus is the major factor in the improved thermal shock resistance of the high E - low E material compared to the thermal shock resistance of the high E material alone.

The ratios of modulus of rupture over Young's modulus were calculated. These calculated values are shown in Table IV. Figures 18 and 19 show the ratio of modulus of rupture to Young's modulus plotted against volume fraction graphite and against volume fraction graphite plus porosity. An increase in the ratio of modulus of rupture over Young's modulus is evident.

5. Thermal Conductivity

No thermal conductivity measurements have been made. The equipment is now constructed and standard samples are being prepared.

6. Thermal Shock

Thermal shock tests as described under equipment were carried out. For the one-inch spheres results were negative insofar that under no condition of thermal shock could these be fractured. Even quenching from $1500^\circ C$. into water at room temperature failed to cause fracture. This can be explained by the fact that the relatively small size of the sphere causes Biot's modulus to be so small that the temperature difference necessary to cause fracture is larger than the temperature difference to which the spheres were subjected.

Spheres of two inch diameter, composed of zirconium carbide without graphite fractured when subjected to thermal shock by heating at a furnace temperature of $1350^\circ C$. The time to fracture was estimated to be 15 seconds. Typical thermal shock fragments are shown in Figure 20. Spheres containing various volume fractions of graphite are now being manufactured. The temperature difference necessary to fracture these will be determined and compared with the results obtained for the ratio of strength over Young's modulus.

7. Internal Stresses

Experiments were undertaken to measure the lattice strain of the graphite in the zirconium carbide-graphite body in order to determine the magnitude of the stresses present. The lattice parameter (c-spacing) of the strained graphite were measured by means of x-ray diffraction measurements and compared with the c-spacing of the same graphite in the unstrained state. Preliminary results indicated that no measurable lattice strains existed, as no changes in the c-spacings could be detected.

As these lattice strain measurements were limited to crystallographic planes parallel to the surface, an attachment to the x-ray goniometer is now being constructed, identical to the attachment used by Fulrath,[21] by means of which the Geiger tube can be positioned accurately. This will allow measurement of lattice spacings oriented at an angle to the specimen surface.

8. Poisson's Ratio

    Resistance strain gauge experiments are underway to determine the value of Poisson's ratio by other means. Poisson's ratio as determined by the sonic method has consistently been found to be approximately 0.18. The National Bureau of Standards, however, reports a value of 0.25. A complete check of our method and accuracy of our calculations indicates that the value of 0.18 is correct. Determining Poisson's ratio by strain gauge measurement will provide another independent check.

V. CONCLUSIONS

    As was predicted originally, the improvement of thermal shock resistance by the additions of a low E phase is due to the resulting increase in the ratio of strength over Young's modulus. This increase in the ratio of strength to Young's modulus has been demonstrated experimentally. The coefficient of expansion is independent of graphite content, if the high E phase remains continuous; Young's modulus follows the relationship calculated by MacKenzie[6]; strength follows the relationship $S = S_0 (1-K\phi)$ as derived previously. From the experimental data available, the constant K can be calculated to be approximately 1.4, which indicates that strength is controlled mainly by the projected cross-sectional area of the included low E particles. The overall result is an increase in the ratio S/E with increasing additions of the low E phase (Table VI).

    The hypothesis that the graphite may be regarded as porosity has been substantiated by experiment. Plotting Young's modulus as a function of graphite plus porosity content follows the relationship calculated by MacKenzie[6]. Especially good agreement at high graphite content shows the graphite to be equivalent to spherical porosity. However, plotting modulus of rupture against graphite plus porosity content does not give a smooth relationship, the high porosity bodies consistently being low in strength. The microstructure of the zirconium carbide in bodies of high porosity will differ from that of bodies containing particles of graphite. The equidimensional shape of the graphite particles approximates spherical porosity, while the pores can be any shape ranging from spherical to tabular. In the case of hot-pressed materials, the tabular pores are favored; therefore, the high porosity materials exhibit lower strength than predicted.

It is concluded that the only role of the low E phase in the composite material is to control pore shape during densification. Its role in influencing the mechanical properties of the final product is equivalent to spherical porosity.

The initial assumption that Young's modulus follows the same relationship as the shear modulus as calculated by MacKenzie[6] has been shown to be valid. Poisson's ratio remains nearly constant with variation in graphite content within experimental limits. The equation relating Young's modulus to the shear modulus is given by

$$G = \frac{E}{2(1+\nu)}$$ which for constant ν gives $\frac{dE}{E} = \frac{dG}{G}$.

The relative increase attainable in the ratio of strength to Young's modulus at high graphite content is at least fifty percent. The actual increase in thermal shock resistance expressed in terms of the additional temperature interval to which a ceramic body can be subjected will depend on the thermal shock resistance of the starting material. The additional temperature to which a material with exceedingly poor thermal shock resistance can be subjected will still be small. The additional temperature to which a good thermal shock resistant ceramic can be subjected can raise the total temperature difference to a value which will exceed the value for a thermal shock of given severity. This then will cause the body to survive.

Additional temperature differences of orders of magnitude can be obtained if thermal shock occurs for cases where Biot's modulus is small enough such that the temperature difference to which the starting material can be subjected is already high.

It is clear that the starting material to which the low E dispersed phase is added should have a low coefficient of thermal expansion, high strength, and as low a Young's modulus as possible.

No conclusions can be drawn concerning the temperature dependence of the ratio of strength to Young's modulus. No measurements have been made of Young's modulus as a function of temperature. However, it may be noticed that the strength of the high-graphite mixtures is nearly independent of temperature as compared with pure zirconium carbide, which is strongly temperature dependent. The indication is that additions of graphite not only improve the ratio of strength over Young's modulus at room temperature, but also that this ratio remains constant or increases with temperature.

The maxima which occur in the modulus of rupture vs. temperature curves may be explained by the presence of internal stresses. As discussed under strength, the zirconium carbide is under tension due to the differences in coefficients of thermal expansion.

An increase in temperature will relieve these internal stresses and will result in an apparent increase in bulk strength. The fact that the increase in strength persisted after annealing indicated that the mechanism responsible is a permanent one. It may also be explained in part that the strength and Young's modulus of the included graphite particles increases with increasing temperatures, thereby increasing the strength of the composite body.

VI. FUTURE WORK

In order to draw final conclusions in this investigation, the following measurements are required:

1. Thermal conductivity measurements as a function of graphite content and temperature.

2. Young's modulus measurements at high temperatures to determine the dependence of the ratio of strength to Young's modulus on temperature.

3. Additional high temperature modulus of rupture measurements to allow statistical treatment of the data.

4. Thermal expansion measurements at high graphite content.

5. Thermal shock tests on two-inch spheres to correlate the experimental data obtained for the individual material properties with the actual thermal shock resistance.

When sufficient data are available, a computer program can be set up to show the effects of each variable, isolated from all others. For example, curves can be plotted to show the effect of porosity at a constant graphite content on strength, Young's modulus and conductivity; likewise the effect of graphite content at a constant porosity as well as at theoretical density.

REFERENCES

1. C. E. Shulze, F. A. Saulino, et al., "Development and Evaluation of Materials for High Temperature Applications," WADC-TR-59-10.

2. W. D. Kingery, "Note on Thermal Expansion and Microstresses in Two-Phase Compositions," J. of Amer. Ceram. Soc., 40, 351 (1957).

3. R. L. Coble, "Effect of Microstructure on Mechanical Properties of Ceramic Materials," Ceramic Engineering Processes, pp. 213-228, John Wiley and Sons, New York, 1957.

4. B. Paul, "Prediction of Elastic Constants of Multiphase Materials," Transactions of A.I.M.E., 218, 37-41 (1960).

5. Jane M. Dewey, "The Elastic Constants of Materials Loaded with Non-Rigid Fillers," J. of App. Physics, 18, 578 (1947)

6. J. K. MacKenzie, "The Elastic Constants of a Solid Containing Spherical Holes," Proc. Phys. Soc. (London) B63, 2-11 (1950).

7. J. N. Goodier, "Concentration of Stress Around Spherical and Cylindrical Inclusions and Flaws," J. Appl. Mech., 1, 39-44 (1933)

8. L. H. Donnell, "Stress Concentrations Due to Elliptical Discontinuities in Plates Under Edge Forces," Theodore V. Karman Anniversary Volume, California Institute of Technology, Pasadena, California, 1941.

9. R. H. Edwards, "Stress Concentrations Around Spheroidal Inclusions and Cavities," Trans. A.S.M.E., 73, 19-30 (1951).

10. B. Paul, "A Note on the Yield-Strength of a Ductile Matrix with Dilute Concentrations of Rigid Inclusions," Department of the Navy, Office of Naval Research, Contract Nonr 562(19) NR 039-028, Technical Report No. 5, May 1960, Division of Engineering, Brown University, Providence, Rhode Island.

11. K. Robinson, "Elastic Energy of an Ellipsoidal Inclusion in an Infinite Solid," J. App. Physics, 22, 1045 (1951).

12. R. H. Edwards, "Stress Concentrations Around Spheroidal Inclusions and Cavities," Trans. A.S.M.E., 73, 19 (1951).

13. J. Gurland, "Temperature Stresses in the Two-Phase Alloy System WC-Co," Trans. A.S.M. 50 (1958).

14. J. Gurland, "Variation of Residual Microstresses with Composition of Two-Phase Alloys, " Department of the Navy, Office of Naval Research, Contract Nonr-562 (19), NR 039-028 Technical Report No. 4, December 1959, Division of Engineering, Brown University, Providence, Rhode Island.

15. R. L. Fullmann, "Measurement of Particle Sizes in Opaque Bodies," Trans. A.I.M.E., 197, 447 (1953).

16. W. D. Kingery, "Thermal Conductivity: XIV, Conductivity of Multicomponent Systems," J. of Amer. Ceram. Soc., 42, 617, (1959).

17. A. Eucken, "Wärmeleitfahigkeit Keramischer Feuerfester Stoffe; Berechnung aus der Wärmeleitfahigkeit der Bestandteile, " Forsch. Gebiete Ingenieurw, B.3, Forschungsheft No. 353, 16 pp. (1932). Ceram. Abstr. 12

18. W. B. Crandall and J. Ging, "Thermal Shock Analysis of Spherical Shapes," J. of Amer. Ceram. Soc., 38, 44 (1955).

19. G. Pickett, Equations for Computing Elastic Constants from Flexural and Torsional Resonant Frequencies of Vibrations of Prisms and Cylinders, A.S.T.M. Proc., 45, 846-63 (1945).

20. J. Francl, W. D. Kingery, "Thermal Conductivity: IV, Apparatus for Determining Thermal Conductivity by a Comparative Method," J. Am. Ceram. Soc., 37, 80 (1954).

21. Internal Stresses in Model Ceramic Systems II, Second Technical Progress Report, Directorate of Solid State Sciences, Air Force Office of Scientific Research, ARDC, Washington 25, D.C. Series No. 119. Issue No. 2, Minerals Research Laboratory, University of California, Berkeley.
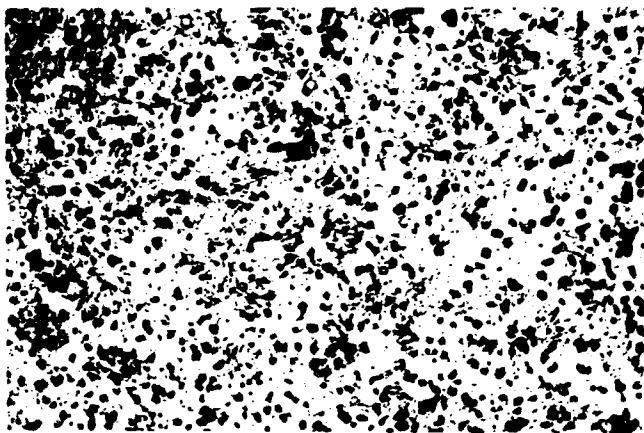
O VOLUME PERCENT GRAPHITE
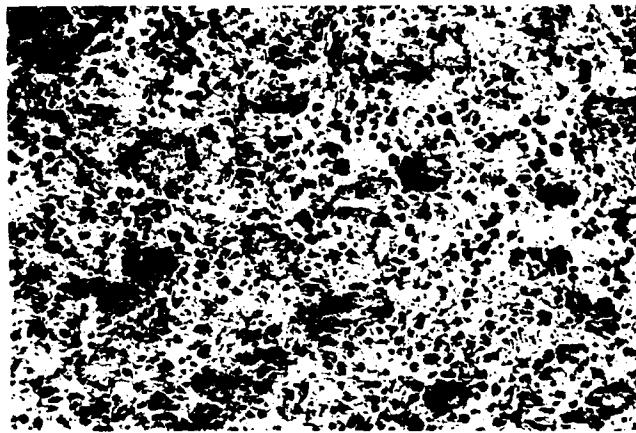
10 VOLUME PERCENT GRAPHITE
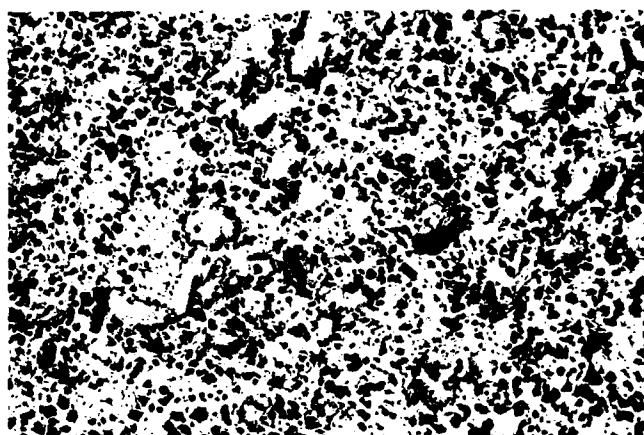
20 VOLUME PERCENT GRAPHITE
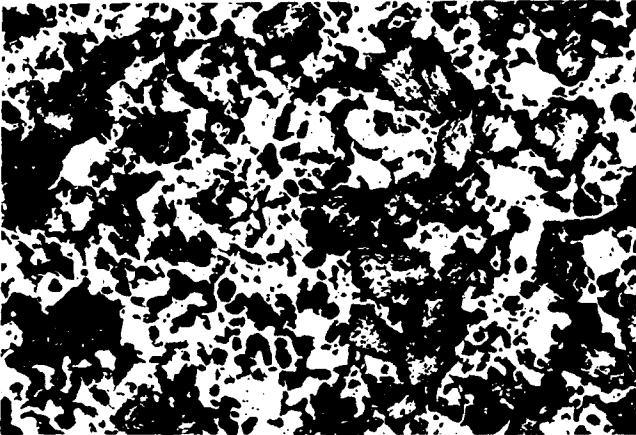
30 VOLUME PERCENT GRAPHITE
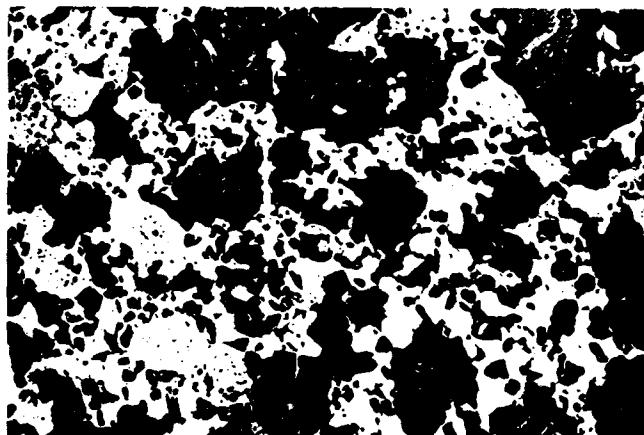
40 VOLUME PERCENT GRAPHITE
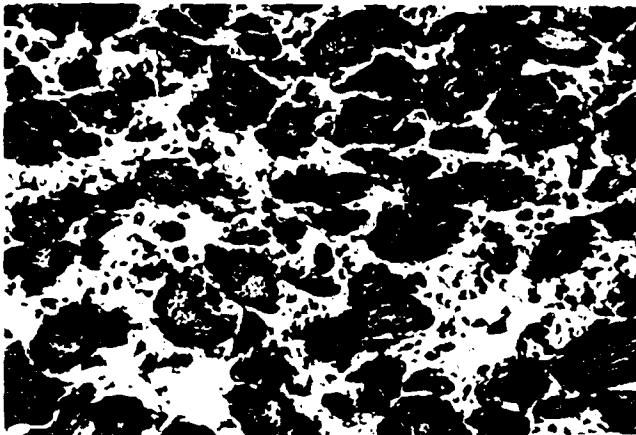
50 VOLUME PERCENT GRAPHITE

Figure 1 - Photomicrographs of polished section of zirconium carbide-graphite samples (x 50).
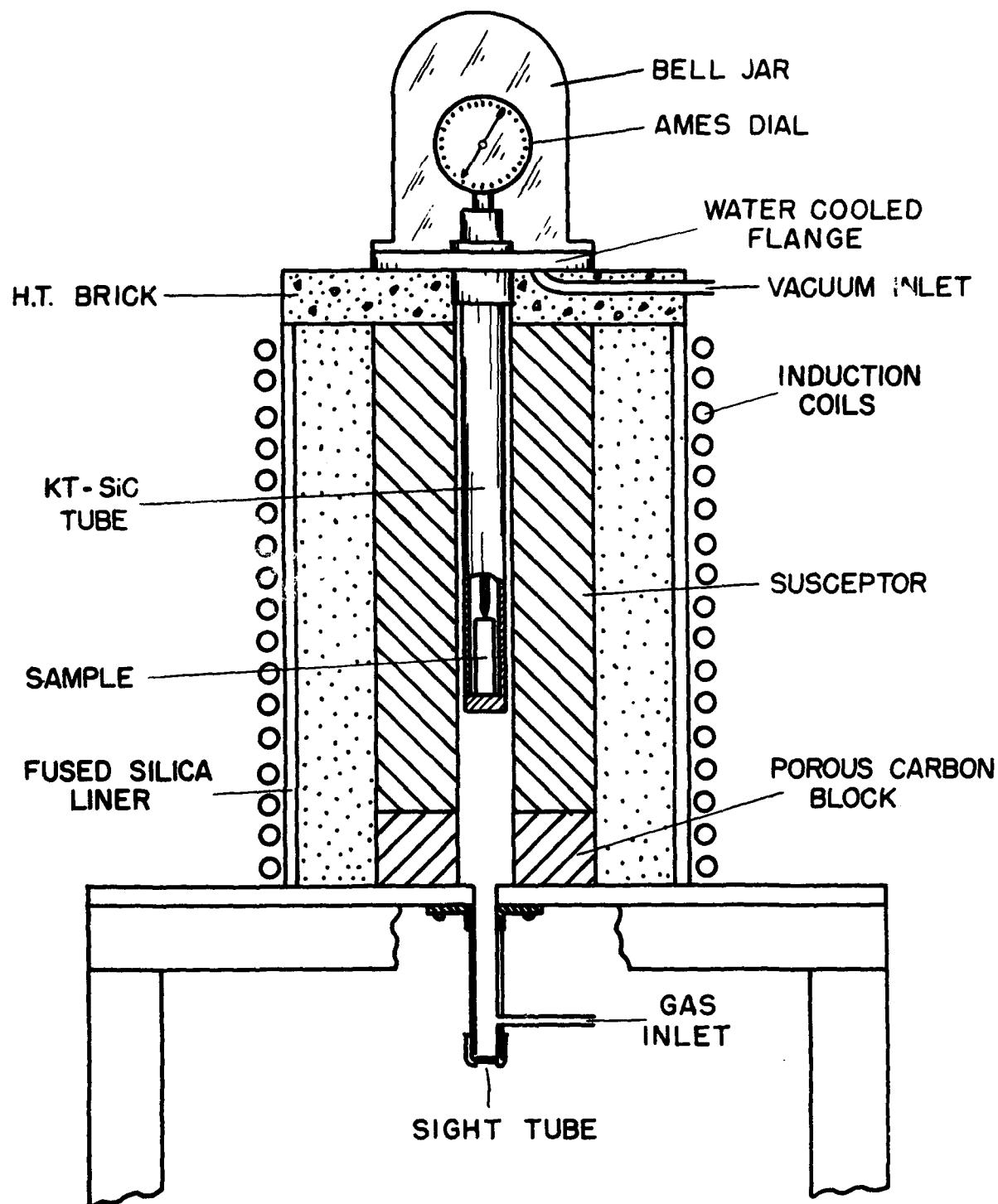
Figure 2 - Induction Heated Inert Atmosphere Dilatometer
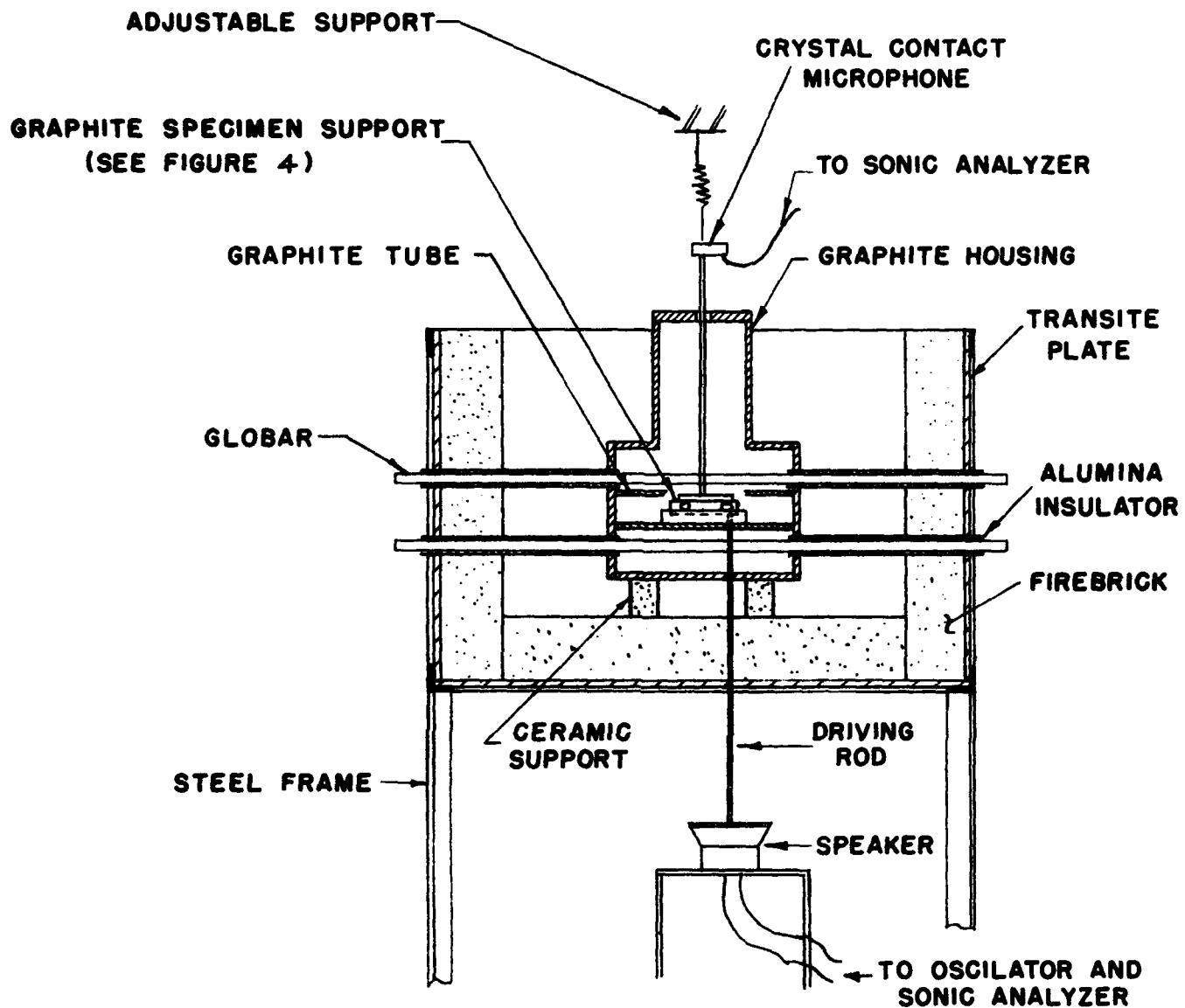
Figure 3 - High Temperature Test Furnace For Sonic Modulus

POSITION OF BOAT FOR TORSIONAL VIBRATION

SLIT FOR DRIVING ROD

HOLES FOR GRAPHITE PINS FOR TORSIONAL VIBRATIONS

TEST BAR

ROD TO CRYSTAL CONTACT MICRO-PHONE

GRAPHITE PINS FOR FLEXURAL VIBRATIONS

HOLE FOR DRIVING ROD
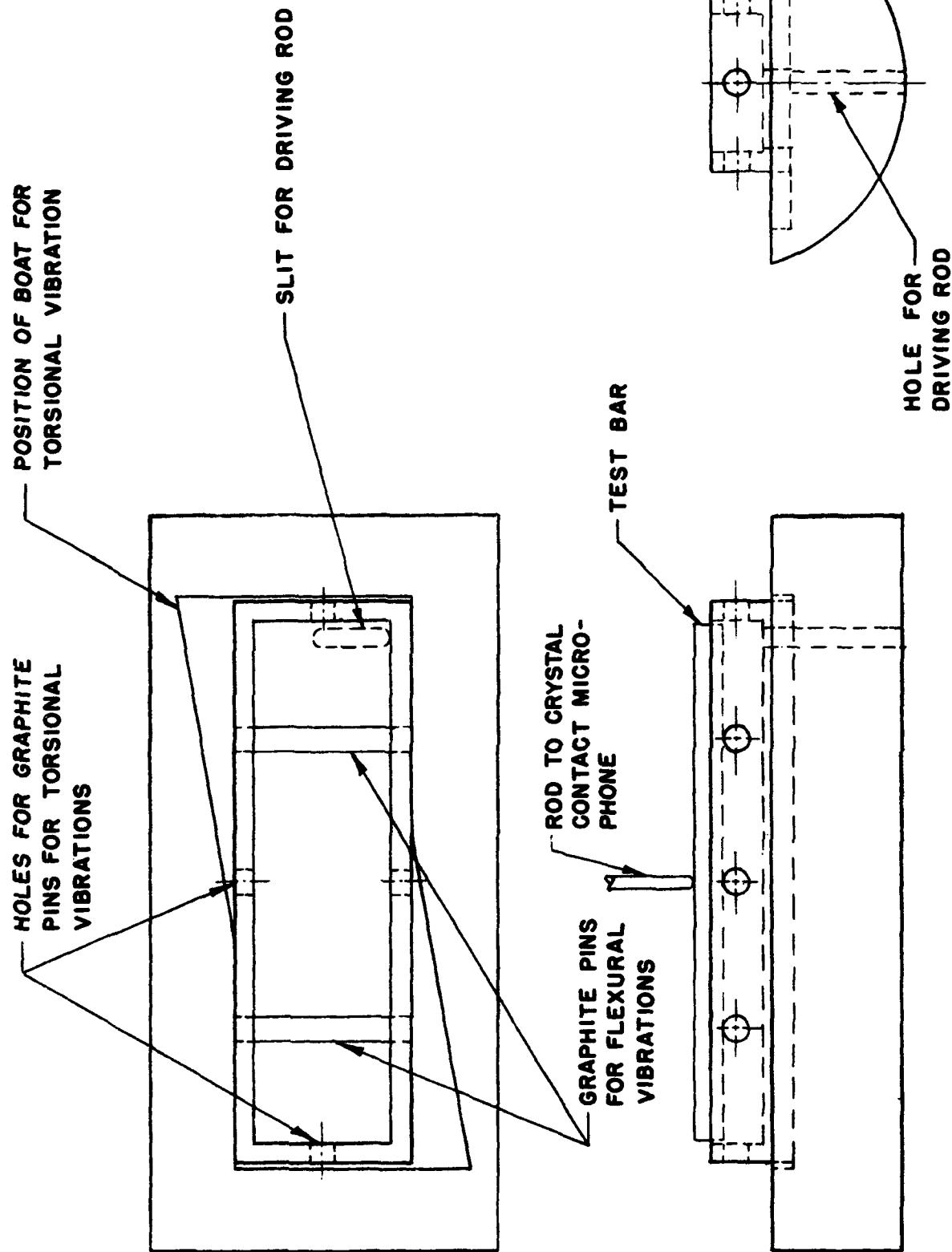
Figure 4 – Test Bar Holder for Measurement of Elastic Constants at High Temperature (Test Bar in Position for Flexural Mode of Vibrations)
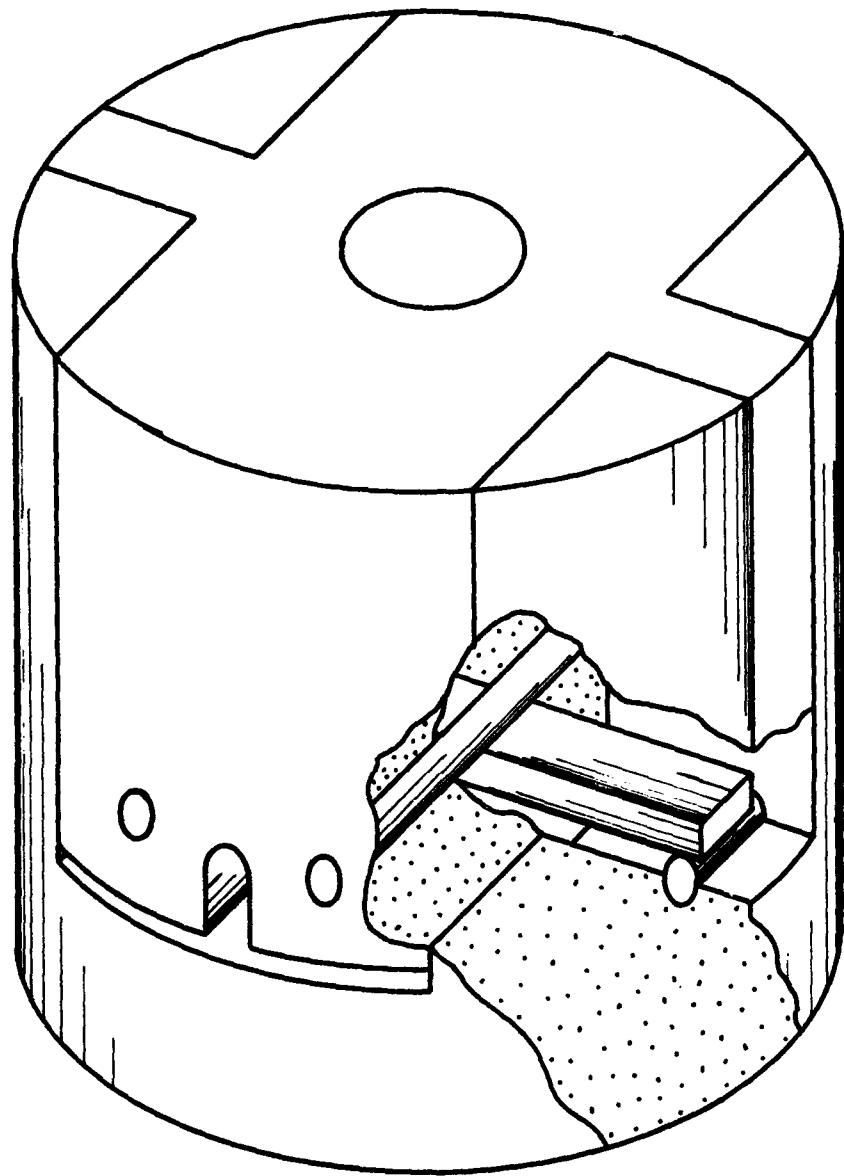
Figure 5 - High Temperature Modulus of Rupture Apparatus
(Cut Away View)
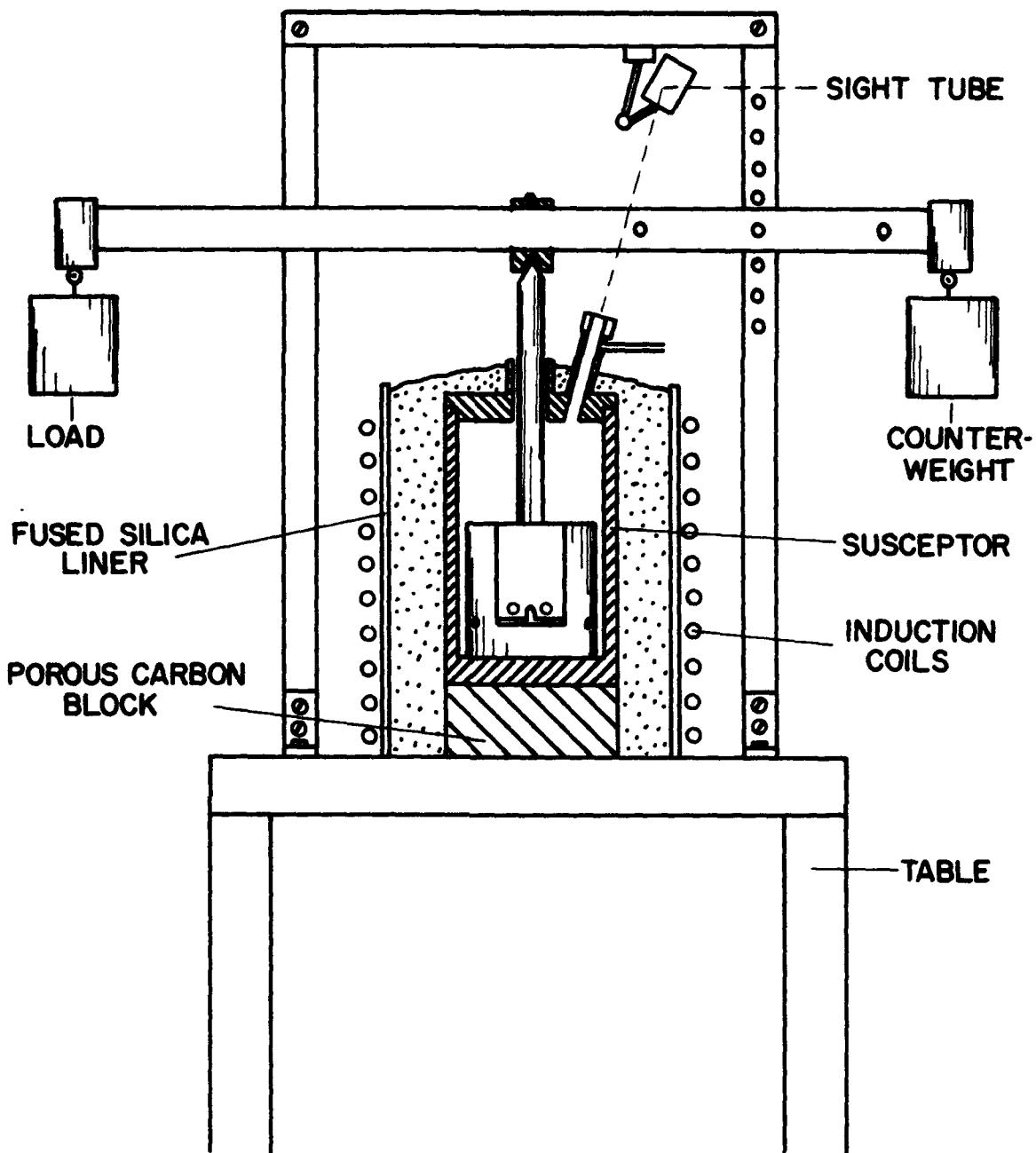
Figure 6 - High Temperature Modulus of Rupture Apparatus

BELL JAR

FURNACE

CONTROL PANEL

SPRING LOADING DEVICE

REMOVABLE PLATE

CERAMIC TUBE

ALUMINA

INSULATION

TRANSITE

STANDARD

SAMPLE

STANDARD

T—THERMOCOUPLE

H—HEATER
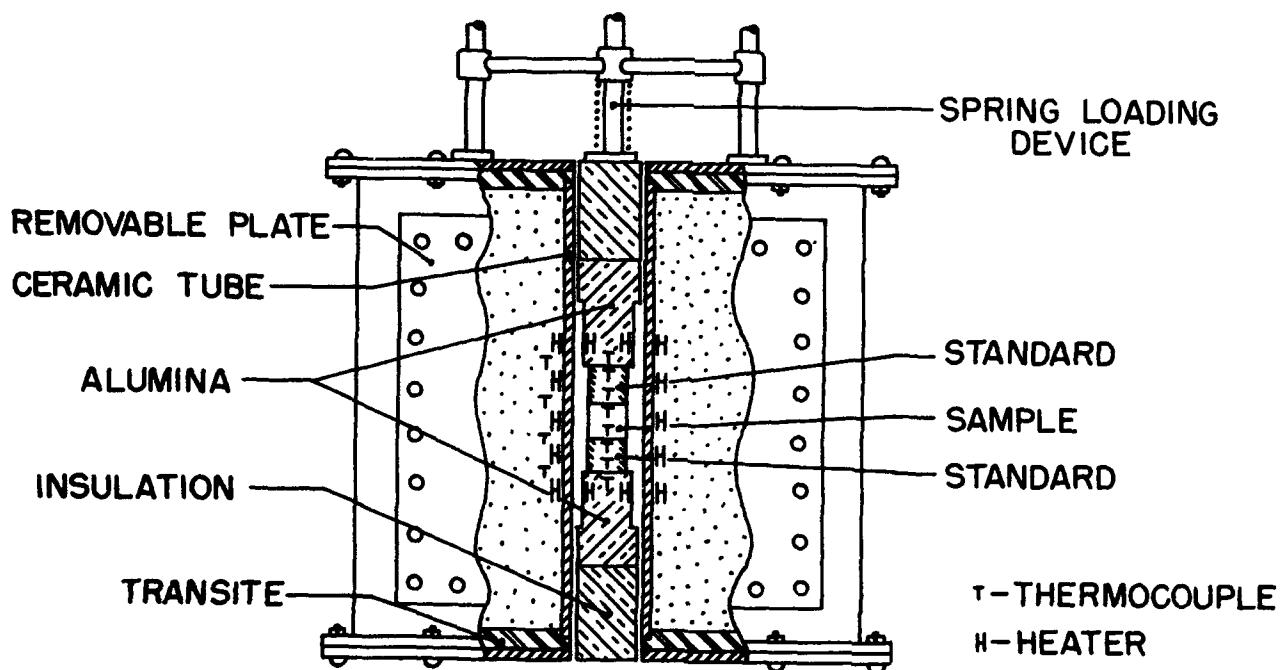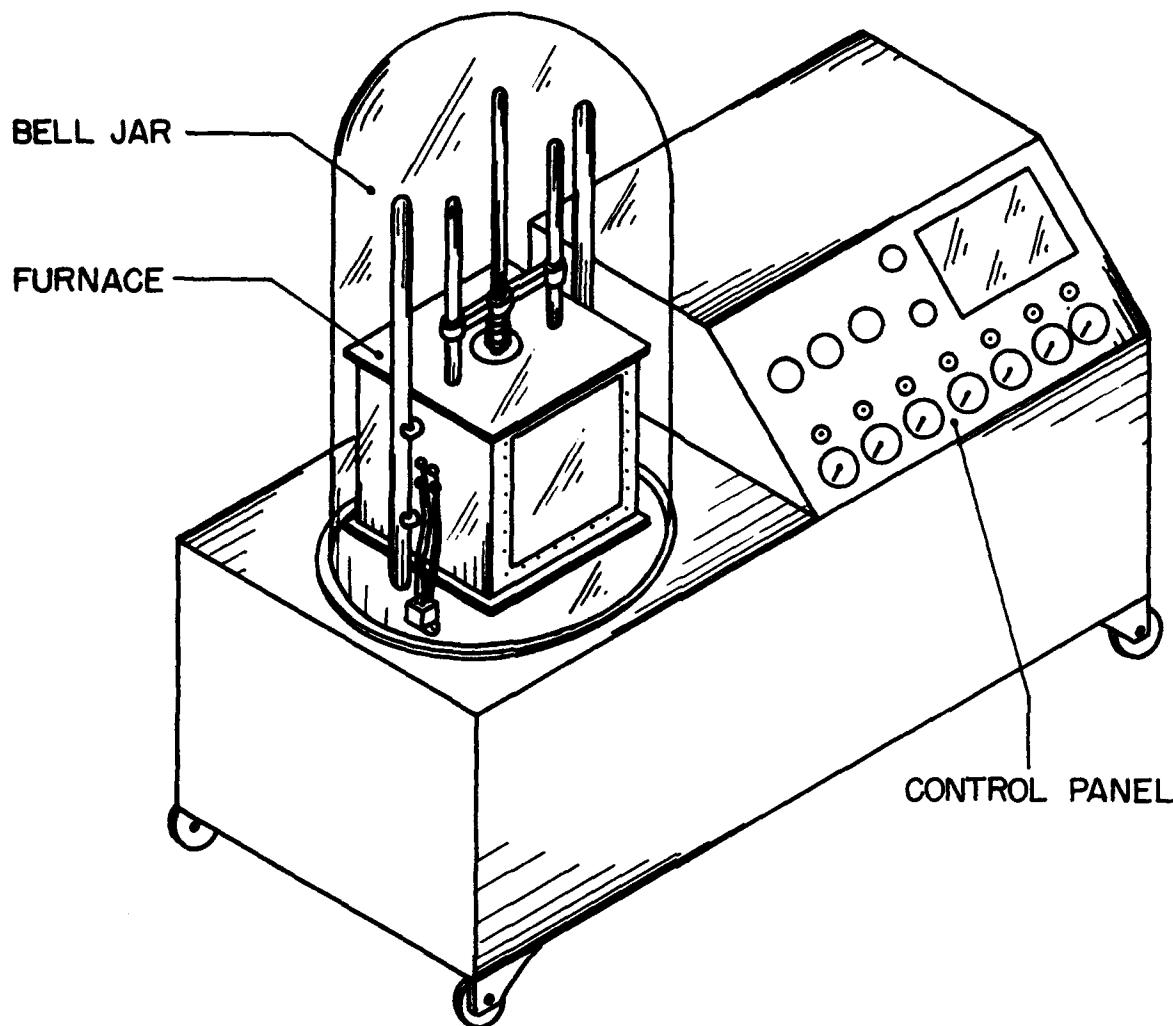
Figure 7 - Thermal Conductivity Apparatus
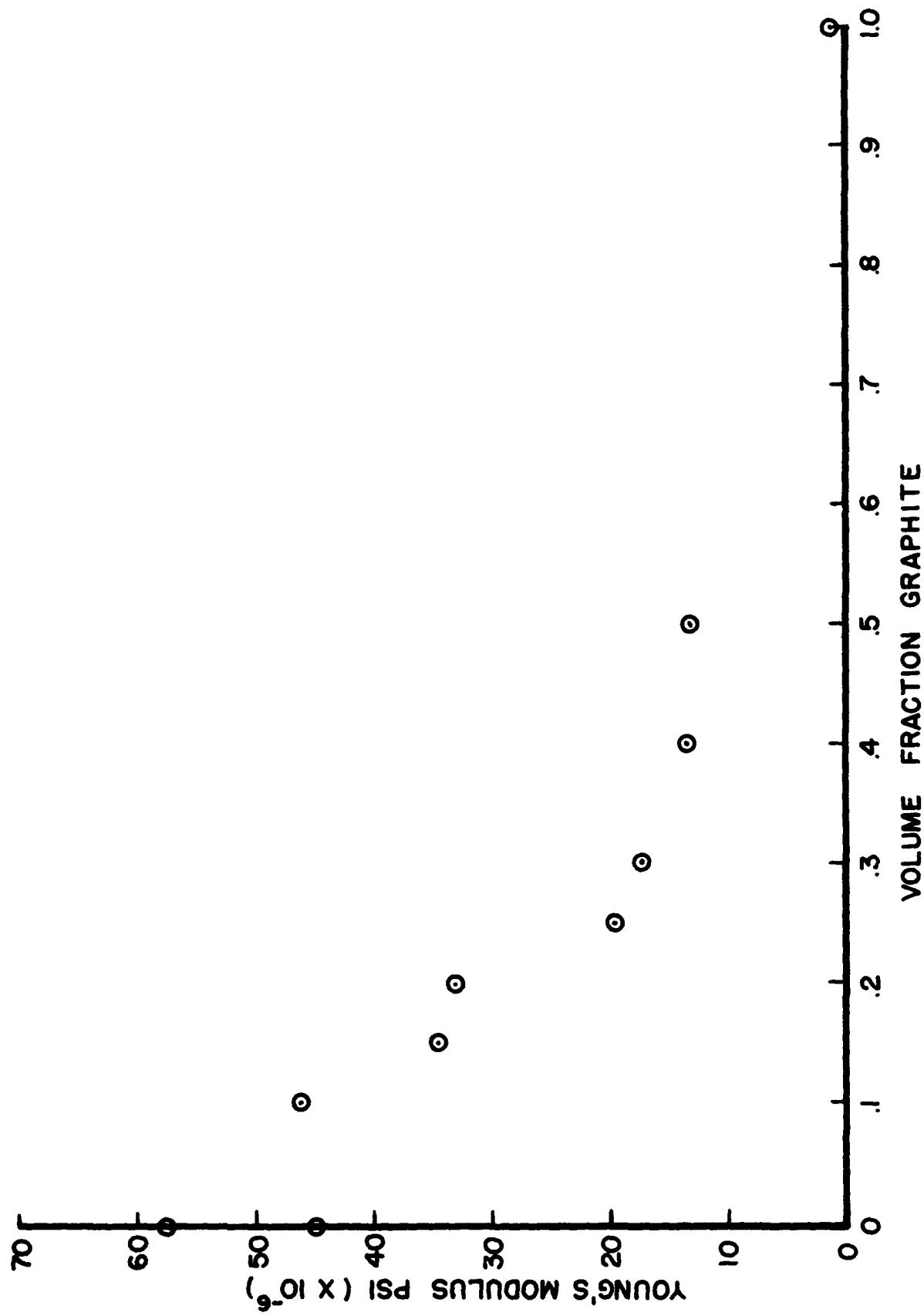
Figure 8 - Young's Modulus of Zirconium Carbide-Graphite (Room Temperature)
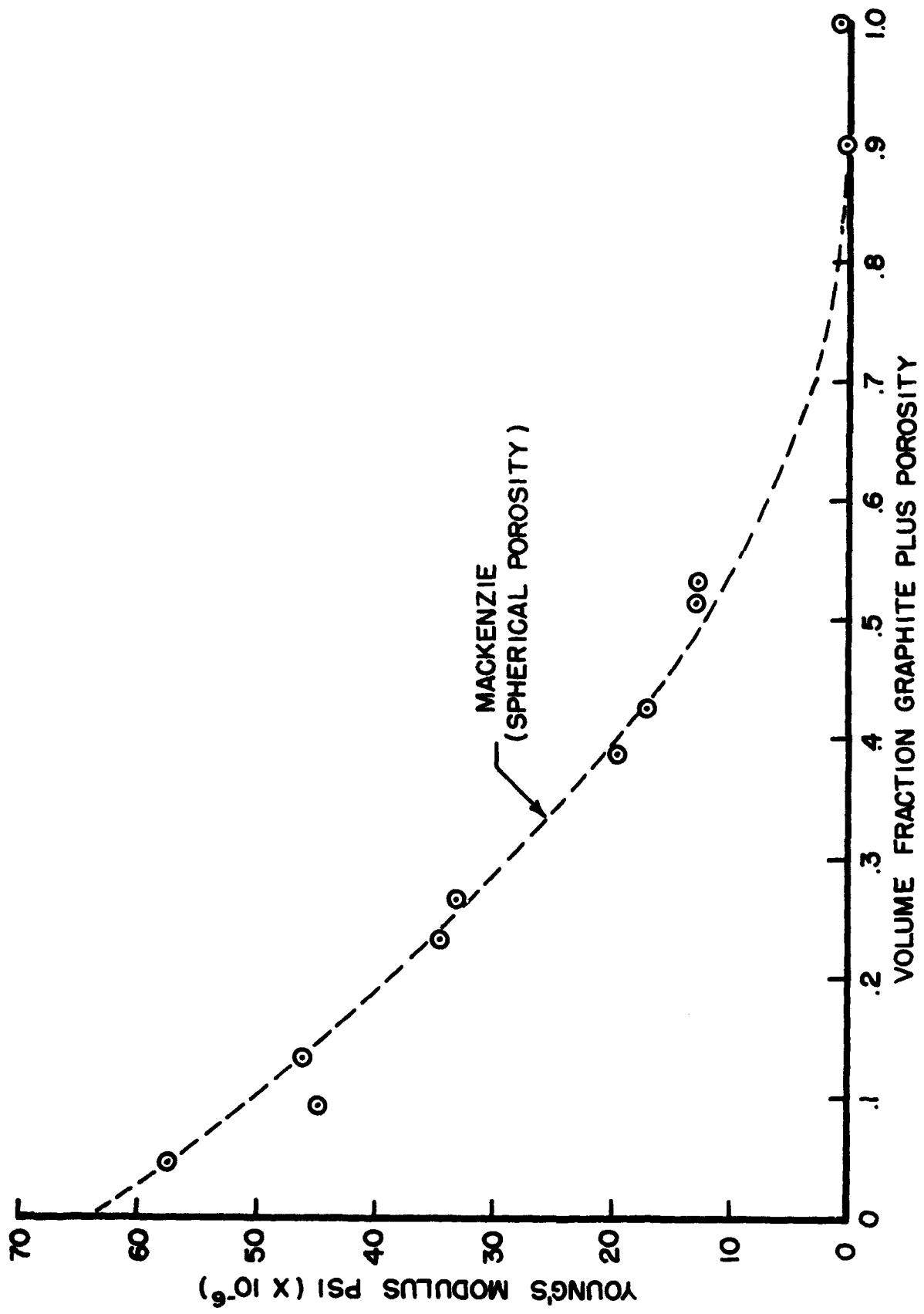
Figure 9 – Young's Modulus of Zirconium Carbide–Graphite + Porosity
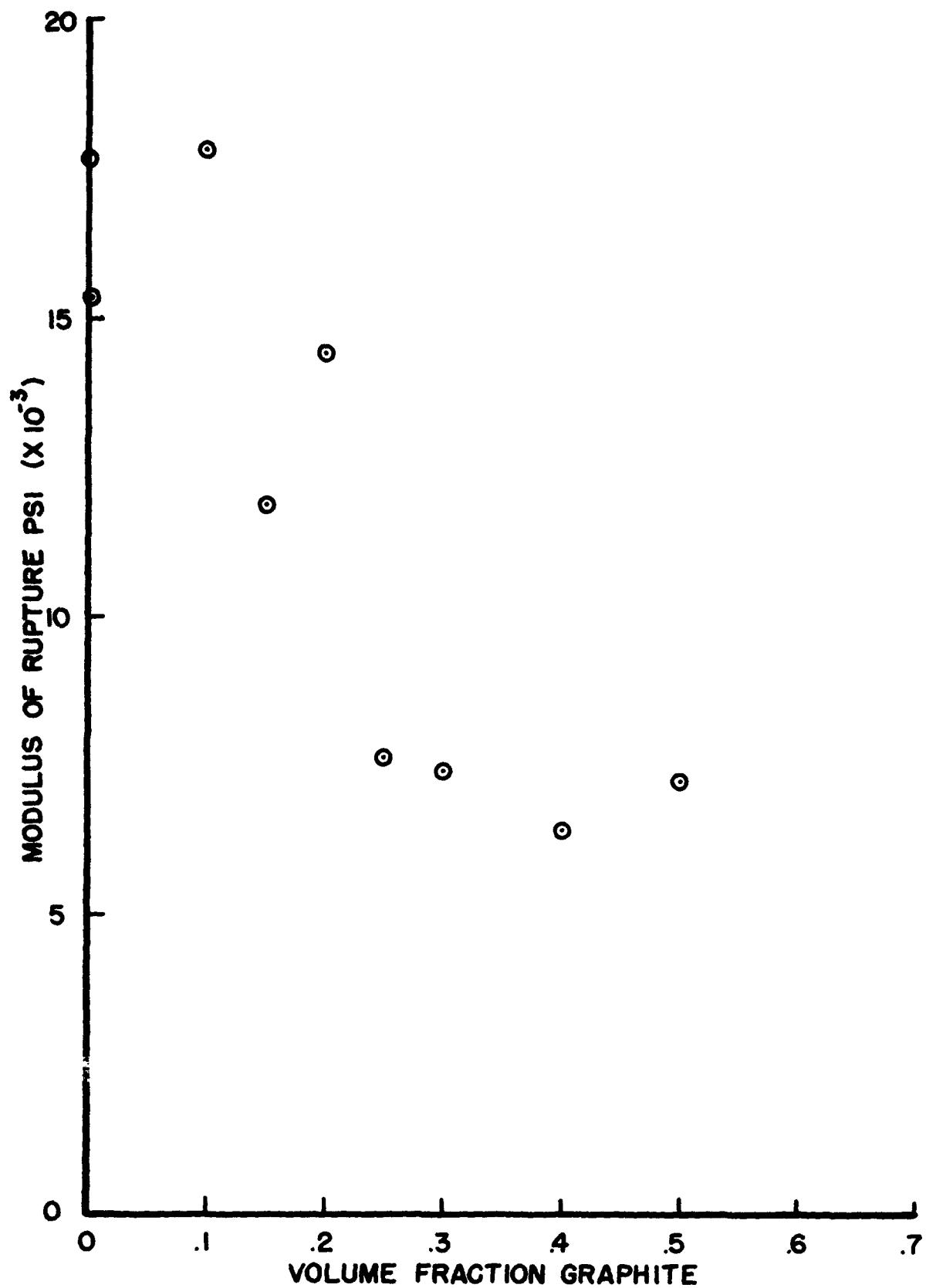
Figure 10 - Modulus of Rupture of Zirconium Carbide-Graphite Against
Graphite Content (Room Temperature)
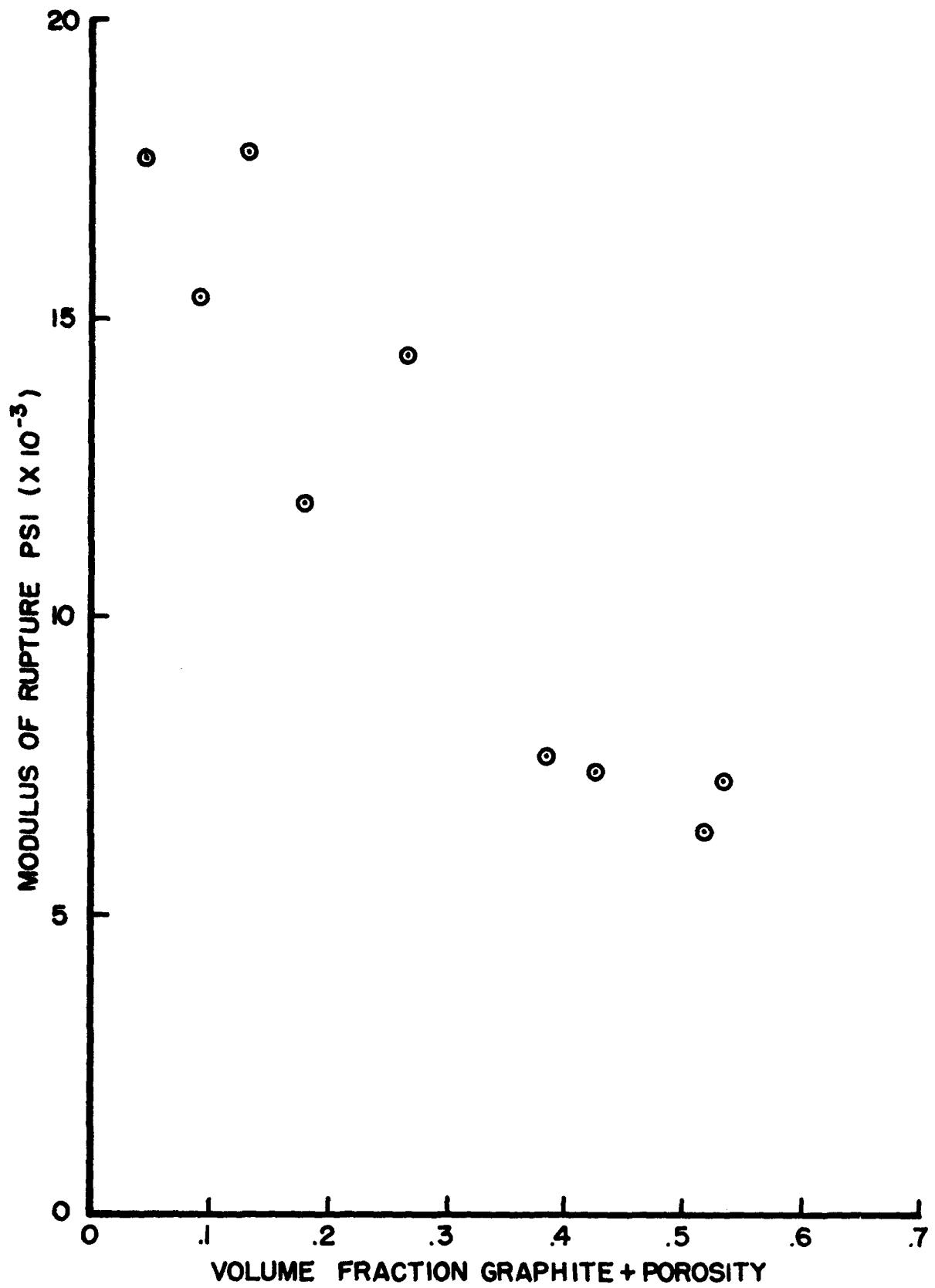
Figure 11 - Modulus of Rupture of Zirconium Carbide - Graphite + Porosity (Room Temperature)
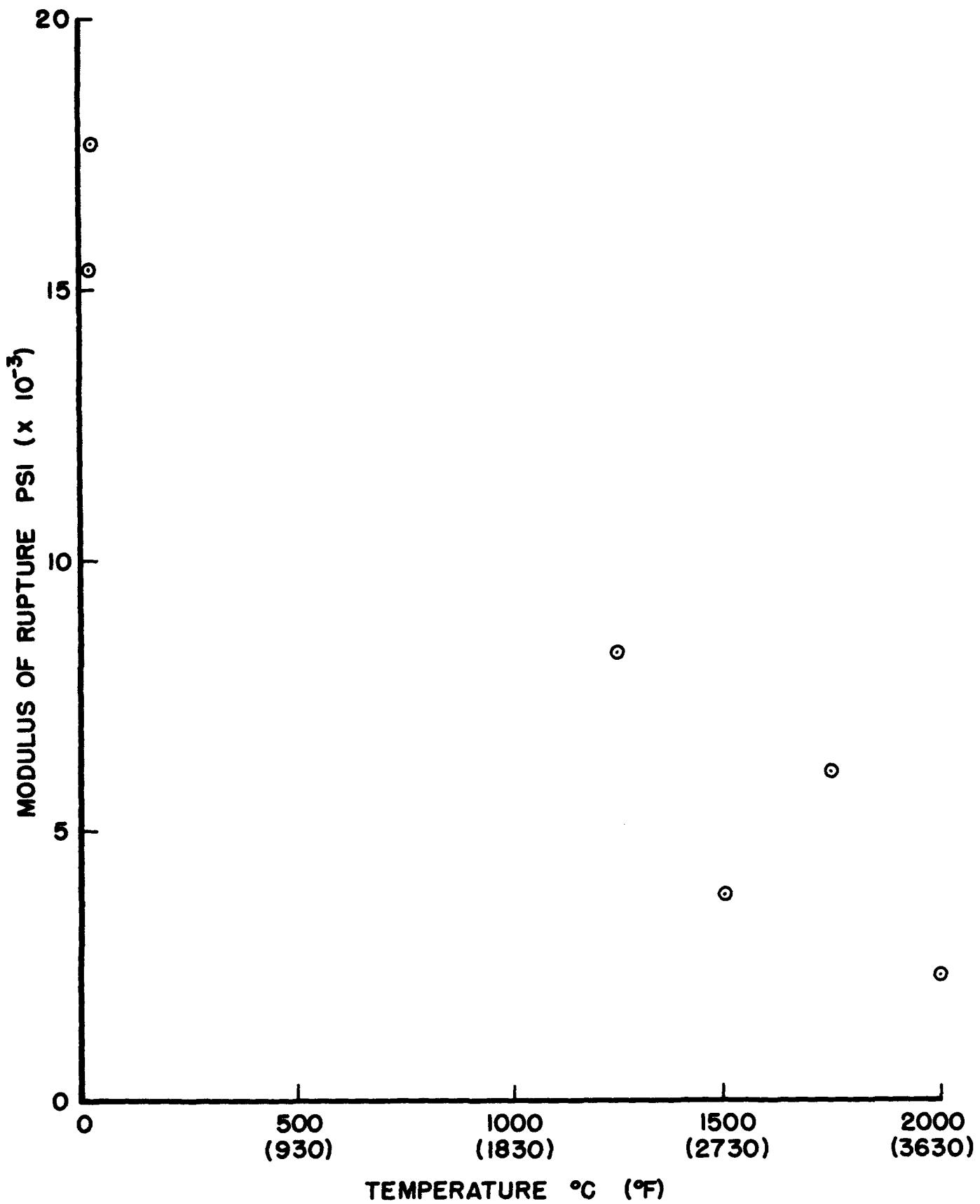
Figure 12 - Modulus of Rupture of Zirconium Carbide vs. Temperature
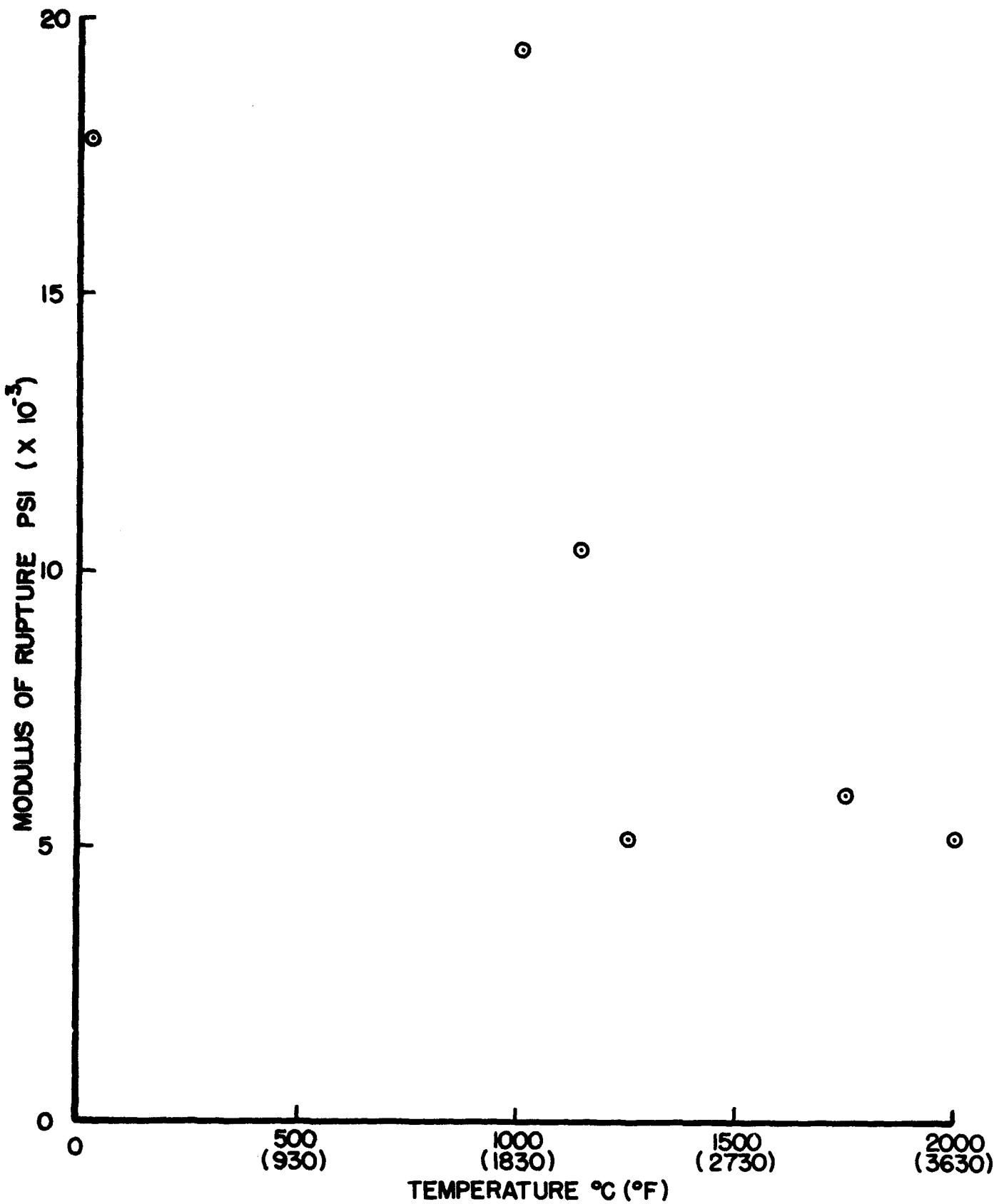
Figure 13 - Modulus of Rupture of Zirconium Carbide
+ Ten Volume Percent Graphite
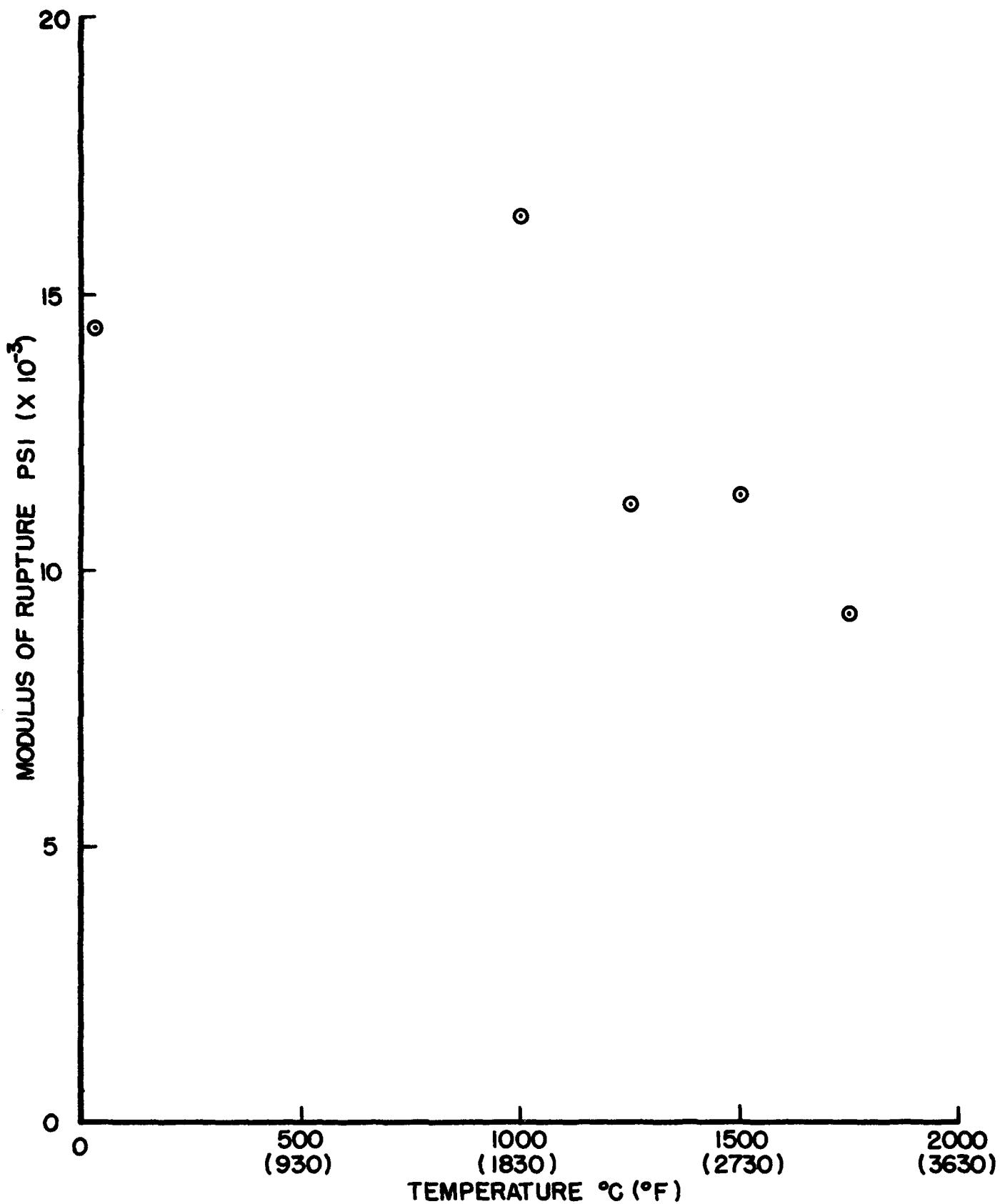
Figure 14 - Modulus of Rupture of Zirconium Carbide
+ Twenty Volume Percent Graphite
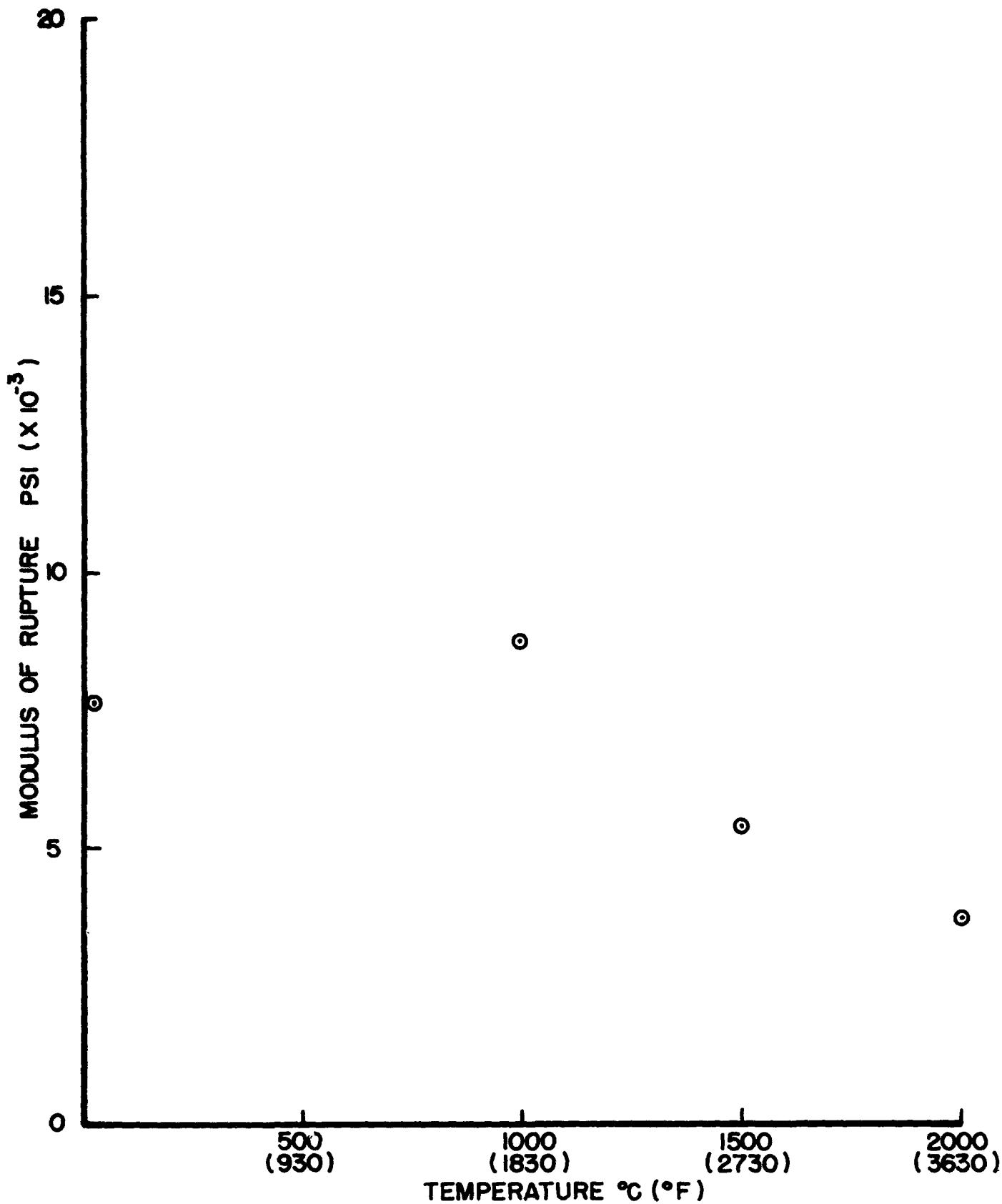
Figure 15 - Modulus of Rupture of Zirconium Carbide +
Twenty Five Volume Percent Graphite
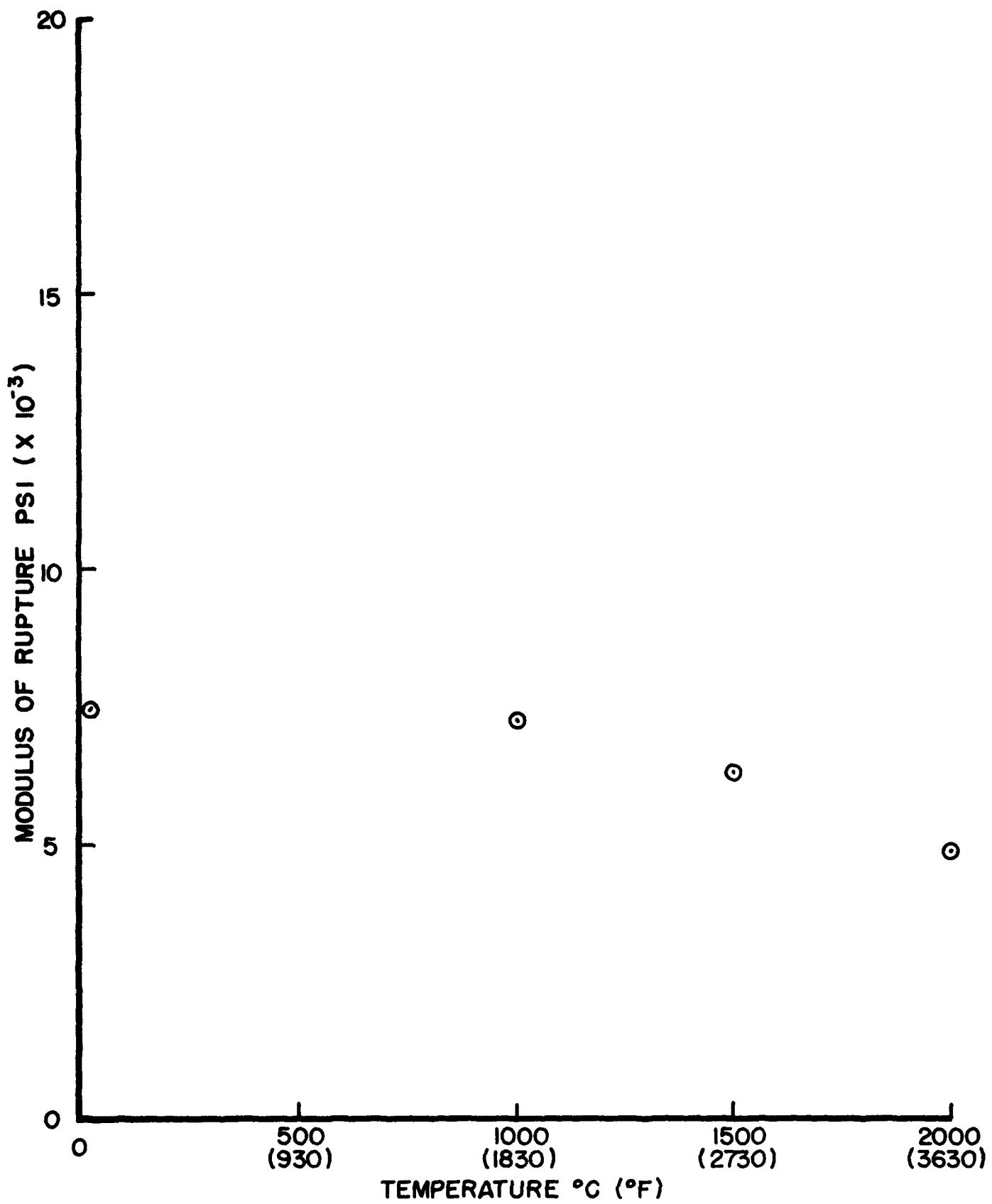
Figure 16 - Modulus of Rupture of Zirconium Carbide
+ Thirty Volume Percent Graphite
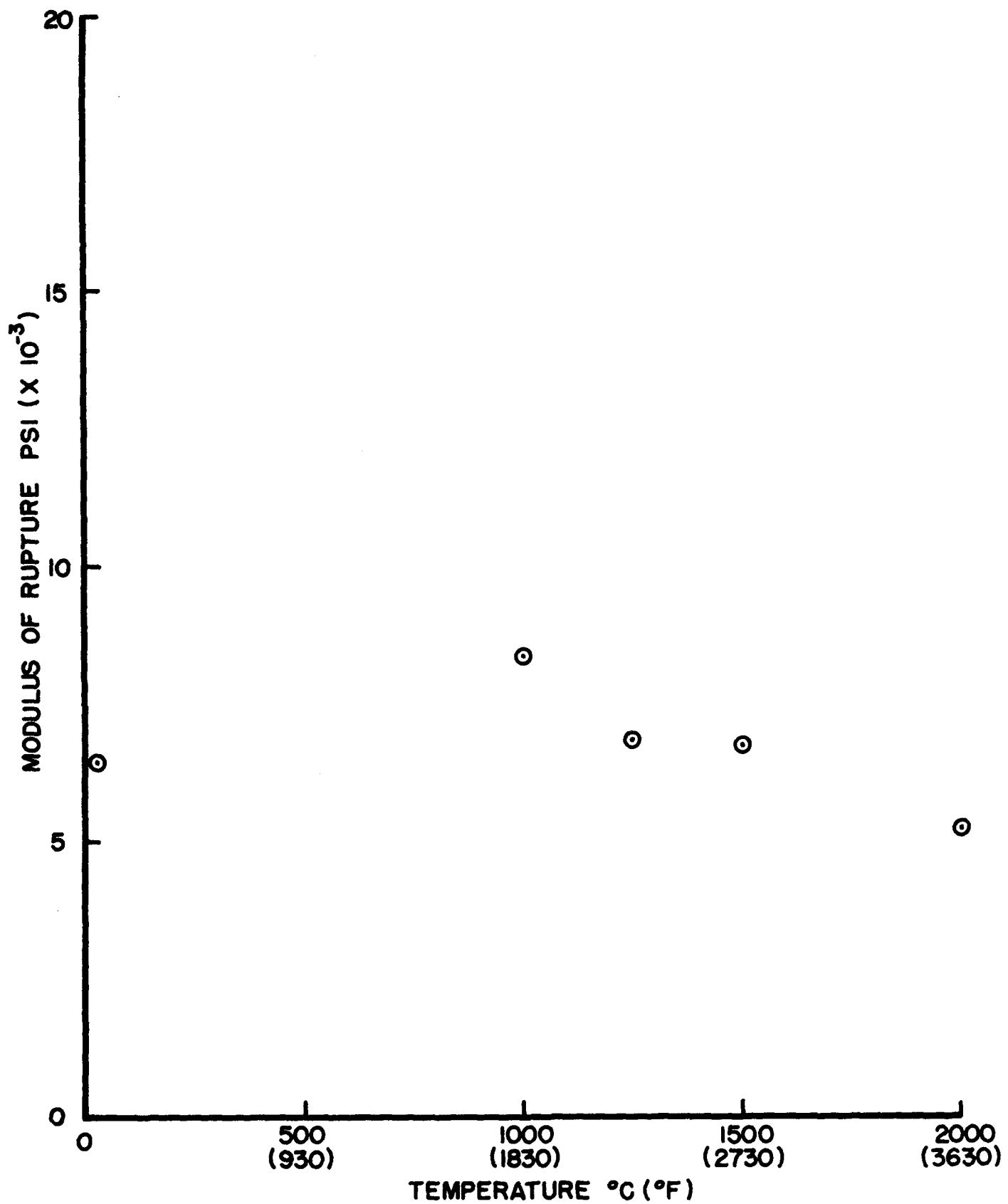
Figure 17 - Modulus of Rupture of Zirconium Carbide
+ Forty Volume Percent Graphite
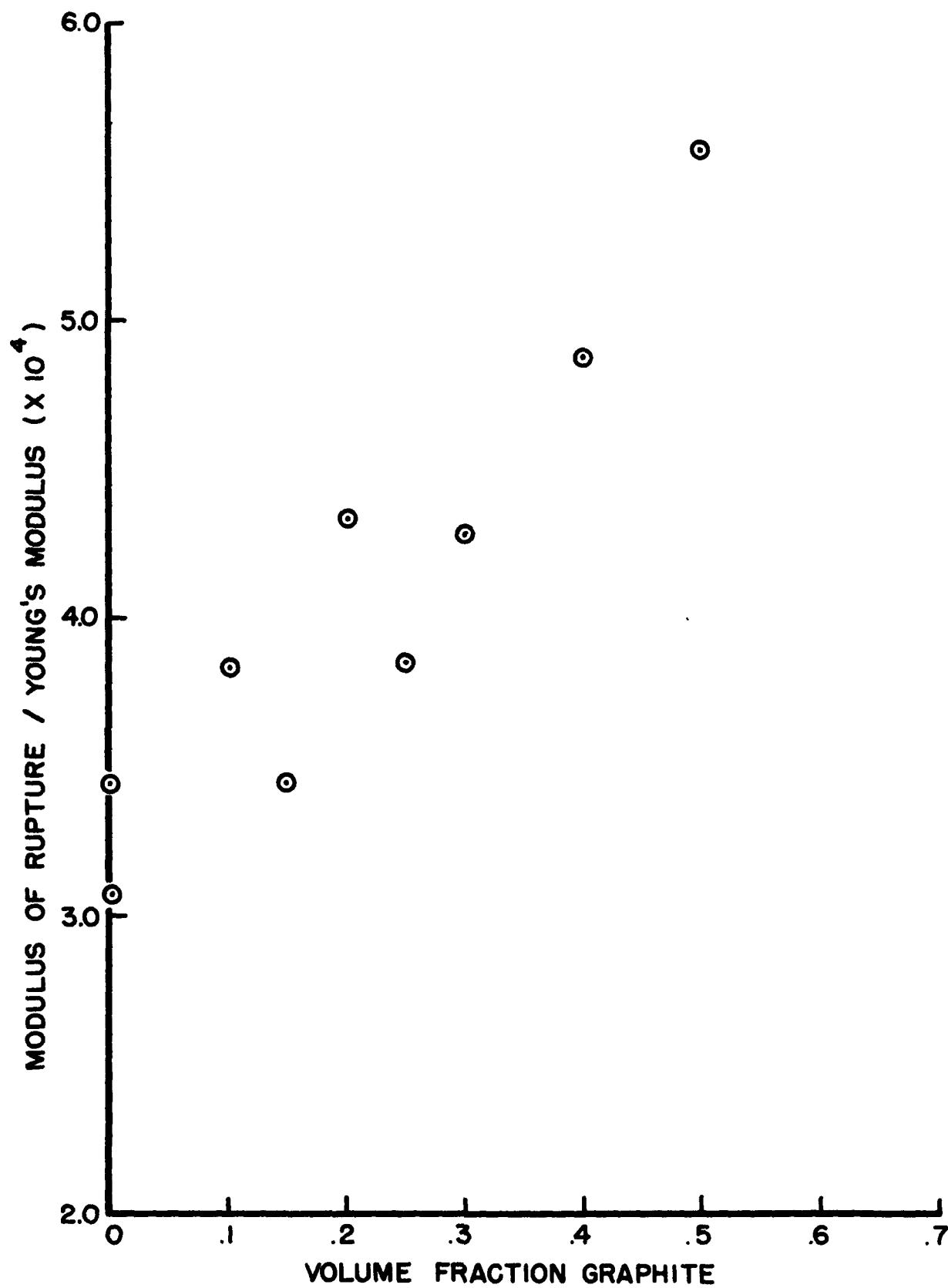
Figure 18 - Ratio of Strength to Young's Modulus of Zirconium
Carbide-Graphite at Room Temperature
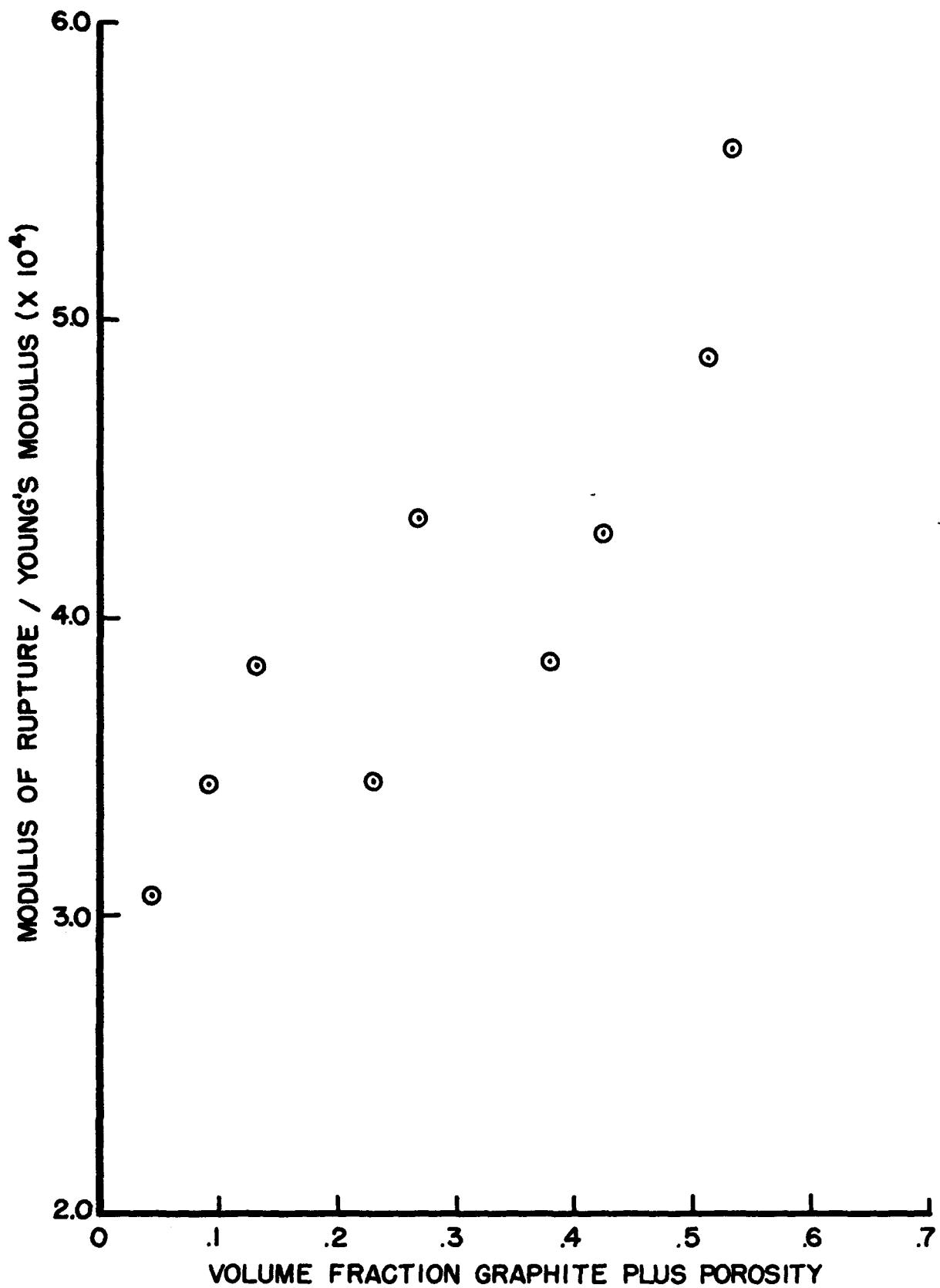
Figure 19 - Ratio of Strength to Young's Modulus of
Zirconium Carbide-Graphite + Porosity
at Room Temperature

Figure 20 - Typical Fragments of Thermally Shocked Zirconium Carbide Spheres.

TABLE NO. I

COEFFICIENT OF THERMAL EXPANSION

Material	Temperature	Range
	1000°C. - 1500°C.	1500°C. - 2000°C.
	(1830°F. - 2730°F.)	(2730°F. - 3630°F.)
ZrC	$10.0 \times 10^{-6}/^{\circ}$C.	$12.4 \times 10^{-6}/^{\circ}$C.
ZrC + 10% Graphite	$10.2 \times 10^{-6}/^{\circ}$C.	$12.2 \times 10^{-6}/^{\circ}$C.
ZrC + 20% Graphite	$10.4 \times 10^{-6}/^{\circ}$C.	$12.4 \times 10^{-6}/^{\circ}$C.

TABLE NO. II

Young's Modulus, Shear Modulus, Poisson's Ratio

Material	Young's Modulus E p.s.i. $(\times 10^{-6})$	Shear Modulus G p.s.i. $(\times 10^{-6})$	Poisson's Ratio	Porosity (%)
ZrC	57.57	24.66	0.167	4.5
ZrC	44.76	-	-	9.1
ZrC (foam)	0.80	-	-	90.6
ZrC + 10% Graphite	46.40	19.79	0.170	3.2
ZrC + 15% "	34.60	14.64	0.180	8.0
ZrC + 20% "	33.29	14.39	0.166	6.5
ZrC + 25% "	19.90	8.54	0.165	13.3
ZrC + 30% "	17.38	7.33	0.186	12.3
ZrC + 40% "	13.16	5.53	0.185	11.3
ZrC + 50% "	13.00	5.38	0.208	3.2

Graphite perpendicular to plane

	0.99	0.45	-	28

Graphite parallel to plane

	1.64	0.54	-	28

TABLE NO. III

MODULUS OF RUPTURE

Material	Temperature °C.	Modulus of Rupture p.s.i.	No. of Specimens Tested
ZrC (9.1% porosity)	25	15,390	4
	1250	8,300	1
	1500	3,800	1
	1750	5,140	1
	2000	2,345	3
ZrC (4.5% porosity)	25	17,700	6
ZrC foam (90.6% porosity)	25	105	1
ZrC + 10% Graphite (3.2% porosity)	25	17,810	8
	880	23,100	1
	1000	19,470	3
	1150	10,300	1
	1250	5,170	2
	1750	5,970	2
	2000	5,170	1
ZrC + 15% Graphite (8% porosity)	25	11,921	11
ZrC + 20% Graphite (6.5% porosity)	25	14,410	9
	1000	16,400	1
	1250	11,250	2
	1500	10,760	2
	1750	9,250	1
	2000	4,050	1
ZrC + 25% Graphite (13.3% porosity)	25	7,670	8
	1000	8,552	1
	1500	5,428	1
	2000	3,375	1

MODULUS OF RUPTURE

Material	Temperature °C.	Modulus of Rupture p.s.i.	No. of Specimens Tested
ZrC + 30% Graphite	25	7,430	5
(12.3% porosity)	1000	7,250	1
	1500	6,200	1
	2000	4,580	1
ZrC + 40% Graphite	25	6,404	4
(11.3% porosity)	1000	8,380	1
	1250	6,850	1
	1500	6,770	1
	2000	5,230	1
ZrC + 50% Graphite	25	7,235	11
(3.2% porosity)	1000	12,525	1
	1500	8,070	1
	2000	4,550	1
Graphite	25	2,780	20
(28% porosity)	2000	3,570	1

TABLE NO. IV

Ratio of Strength to Young's Modulus

Material	Strength/Young's Modulus x 10^4	Porosity %
ZrC	3.07	4.5
Z.C	3.44	9.1
ZrC	1.31	90.6
ZrC + 10% graphite	3.84	3.2
ZrC + 15% graphite	3.45	8.0
ZrC + 20% graphite	4.33	6.5
ZrC + 25% graphite	3.85	13.3
ZrC + 30% graphite	4.28	12.3
ZrC + 40% graphite	4.87	11.3
ZrC + 50% graphite	5.57	3.2

APPENDIX I

Calculation of Relative Difference Between the Shear Modulus of a High Young's Modulus Continuous Phase Material Containing Spherical Particles of a Low Young's Modulus Material or Spherical Holes

The equation for the effective shear modulus $\overline{\lambda}_2$ as calculated by Jane M. Dewey[5] is given by

$$\overline{\lambda}_2 = \lambda_2 \left\{ 1 + \frac{15(\lambda^1_2 - \lambda_2)(\lambda_1 + 2\lambda_2)\phi}{2\lambda^1_2(3\lambda_1 + 8\lambda_2) + \lambda_2(9\lambda_1 + 14\lambda_2)} \right\} \tag{1}$$

where λ^1_1 and λ^1_2 are Lame's constants of the filler material and λ_1 and λ_2 of the medium, λ_2 is the modulus of rigidity and λ_1 is defined by

$$\lambda_1 + 2/3\,\lambda_2 = k^{-1} \tag{2}$$

where k is the compressibility. ϕ is the volume fraction of the dispersed phase.

Equation (1) can be rewritten into: (3)

$$\overline{\lambda}_2 = \lambda_2 \left\{ 1 + \frac{15(\lambda_1 + 2\lambda_2)(\lambda^1_2 - \lambda_2)\phi}{\lambda_2(9\lambda_1 + 14\lambda_2)\left\{ 1 + \frac{2\lambda^1_2(3\lambda_1 + 8\lambda_2)}{\lambda_2(9\lambda_1 + 14\lambda_2)} \right\}} \right\}$$

The factors $\dfrac{15(\lambda_1 + 2\lambda_2)}{9\lambda_1 + 14\lambda_2}$

and $\dfrac{2(3\lambda_1 + 8\lambda_2)}{(9\lambda_1 + 14\lambda_2)}$

can be calculated, and are approximately equal to 2 and 1 respectively. Substitution of these values into the equation (3) and defining $k_0 = \dfrac{\lambda^1_2}{\lambda_2}$

the ratio of the shear moduli of the filler and matrix material yields

$$\bar{\lambda}_2 = \lambda_2 \left\{ 1 - \frac{2(1-K_0)}{(1+K_0)} \phi \right\} \tag{4}$$

By writing $\dfrac{1}{1+K_0} \approx 1 - K_0$ for $K_0 \ll 1$ as is the case for the system under study, equation (4) neglecting terms containing K_0^2, becomes

$$\bar{\lambda}_2 = \lambda_2 \left\{ 1 - 2(1-K_0)(1-K_0)\phi \right\}$$
$$= \lambda_2 \left\{ 1 - 2\phi + 4 K_0\phi \right\}$$

The term $4 K_0 \phi$ gives the relative difference in effective shear moduli between a material containing spherical particles of a material with low Young's modulus and the same material containing the same volume fraction of spherical holes. For the system under study K_0 is approximately equal to 0.02. Therefore, for a volume fraction of spherical particles of 0.1 the relative difference in shear moduli for a material with high Young's modulus containing particles or pores is 4 x 0.02 x 0.1 = 0.008 or 0.8 percent. The same relation will hold for the effective Young's modulus.

Calculation of Relative Difference Between Stress Concentration
Factors For a Low Young's Modulus Spherical
Particle Contained in a High Young's
Modulus Medium, and The Stress
Concentration Factors For
A Spherical Pore
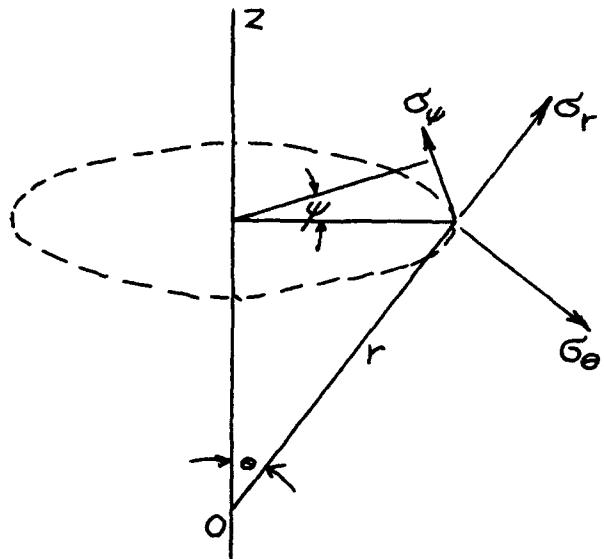
The accompanying figure illustrates the coordinate system for the spherical particle contained in an infinite solid. The center of the particle is taken as the origin. The particle radius is denoted by a. The stress is applied in the Z-direction.

The maximum tensile and compressive stresses occur at the boundary of the particle at $\theta = 0$, π and $\theta = \pi/2$ and are given by:

when $\theta = 0, \pi$

$$\sigma_r = 2\mu_1 \left\{ \frac{2A}{a^3} - \frac{2}{(1-2\nu)} \frac{C}{a^3} + \frac{48B}{a^5} - \frac{2(5-\nu)}{(1-2\nu)} \frac{C}{a^3} + \frac{B}{a^5} \right\}$$

$$\sigma_\theta = 2\mu_1 \left\{ -\frac{A}{a^3} - \frac{2\nu}{(1-2\nu)} \frac{C}{a^3} + \frac{C}{a^5} - 24\frac{B}{a^5} \right\}$$

$$\sigma_\psi = 2\mu_1 \left\{ -\frac{A}{a^3} - \frac{2(1-\nu)}{(1-2\nu)} \frac{C}{a^3} - \frac{24B}{a^5} + \frac{3C}{a^3} \right\}$$

At $\theta = \dfrac{\pi}{2}$ these become:

$$\sigma_r = 2\mu_1 \left\{ \frac{2A}{a^3} - \frac{2\upsilon}{(1-2\upsilon)} \frac{C}{a^3} + \frac{12B}{a^5} \right\}$$

$$\sigma_\theta = 2\mu_1 \left\{ -\frac{A}{a^3} - \frac{2\upsilon}{(1-2\upsilon)} \frac{C}{a^3} - \frac{3B}{a^5} \right\}$$

$$\sigma_\psi = 2\mu_1 \left\{ -\frac{A}{a^3} - \frac{2(1-\upsilon)}{(1-2\upsilon)} \frac{C}{a^3} - \frac{9B}{a^5} \right\}$$

The maximum shear stresses ($\tau_{r\theta}$) occur at $\theta = \dfrac{\pi}{4}$ or $3\dfrac{\pi}{4}$

At $\theta = \dfrac{\pi}{4}$

$$\tau_{r\theta} = 2\mu_1 \left\{ \frac{-2(1+\upsilon)}{(1-2\upsilon)} \frac{C}{a^3} + \frac{24B}{a^5} \right\}$$

At $\theta = \dfrac{3\pi}{4}$

$$\tau_{r\theta} = -2\mu_1 \left\{ \frac{-2(1+\upsilon)}{(1-2\upsilon)} \frac{C}{a^3} + \frac{24B}{a^5} \right\}$$

On the assumption that both materials have the same Poisson's ratio, the constants can be defined as follows:

$$\frac{A}{a^3} = -\frac{T}{8\mu_1}\frac{(\mu_1 - \mu_2)}{(7 - 5\nu)\mu_1 + (8 - 10\nu)\mu_2}$$

$$\times \frac{(1 - 2\nu)(6 - 5\nu)\,2\mu_1 + (3 + 19\nu - 20\nu^2)\mu_2}{(1 - 2\nu)\,2\mu_1 + (1 + \nu)\mu_2}$$

$$+ \frac{T}{4\mu_1}\frac{(1 - 2\nu)\left[\mu_2 - \mu_1\right]}{(1 - 2\nu)\,2\mu_1 + (1 + \nu)\mu_2}$$

$$\frac{B}{a^3} = \frac{T}{8\mu_1}\frac{\mu_1 - \mu_2}{(7 - 5\nu)\mu_1 + (8 - 10\nu)\mu_2}$$

$$\frac{C}{a^3} = \frac{T}{8\mu_1}\frac{5(1 - 2\nu)(\mu_1 - \mu_2)}{(7 - 5\nu)\mu_1 + (8 - 10\nu)\mu_2}$$

In these equations,

μ_1 is the modulus of rigidity of the solid,

μ_2 is the modulus of rigidity of the inclusion,

ν is Poisson's ratio

T   is the applied tension at infinity

a   is the radius of the inclusion.

  Examination of the equations for the stresses reveals that in order to determine the dependence of the stresses on the ratio of the elastic constants, it is sufficient to examine the dependence on the ratio of the elastic properties of the constants A, B and C only.

Letting $K = \mu_1/\mu_2$, the expressions for A, B and C can be rewritten, and rearranged to give:

$$\frac{A}{a^3} = -\frac{T(1-K)}{8(7-5\nu)\mu_1}\left\{1 + \frac{8-10\nu}{7-5\nu}K\right\}$$

$$\times \frac{(6-5\nu)\left\{1 + \frac{(3+19\nu-20\nu^2)}{(1-2\nu)(6-5\nu)}K\right\}}{\left\{1 + \frac{1+\nu}{2(1-2\nu)}K\right\}}$$

$$\frac{T(K-1)}{8\mu_1\left\{1+\frac{1+\nu}{2(1-2\nu)}K\right\}}$$

$$\frac{B}{a^5} = \frac{T}{8}\frac{(1-K)}{(7-5\nu)\mu_1\left\{1+\frac{(8-10\nu)}{7-5\nu}K\right\}}$$

$$\frac{C}{a^3} = \frac{T}{8}\frac{5(1-2\nu)(1-K)}{(7-5\nu)\mu_1\left\{1+\frac{8-10\nu}{7-5\nu}K\right\}}$$

The ratios

$$\frac{3+19\nu-20\nu^2}{(1-2\nu)(6-5\nu)} \quad , \quad \frac{1+\nu}{2(1-2\nu)} \quad \text{and} \quad \frac{8-10\nu}{7-5\nu}$$

can be calculated, and are approximately equal to 5, 2 and 1 respectively for $\nu = 1/3$ and approximately 1 1/2, 1 and 1, respectively for $\nu = 1/6$. Substitution of the values into the previous equations and using the relations:

$$\frac{1}{1 + \propto K} \approx 1 - \propto K \quad \text{for} \ \propto K \ << \ 1 \ \text{and}$$

$(1 + \propto K)(1 + \beta K) \approx 1 + (\propto + \beta) K \ \text{for} \ \propto K, \ \beta K \ << \ 1$
gives for A, B and C:

for $\mathcal{V} = 1/3$,

$$\frac{A}{a^3} = -\frac{T(6 - 5\mathcal{V})(1 + K)}{8\mu_1 (7 - 5\mathcal{V})} - \frac{T(1 - 3K)}{8\mu_1}$$

$$= -\frac{T}{8\mu_1}\frac{(13 - 10\mathcal{V})}{(7 - 5\mathcal{V})} - \frac{T}{8\mu_1}\frac{(15 - 10\mathcal{V})K}{(7 - 5\mathcal{V})}$$

$$\approx \frac{T}{4\mu_1}(1 - K)$$

$$\frac{B}{a^5} = \frac{T(1 - 2K)}{8(7 - 5\mathcal{V})\mu_1}$$

$$\frac{C}{a^3} = \frac{T}{8\mu_1}\frac{5(1 - 2\mathcal{V})}{(7 - 5\mathcal{V})}(1 - 2K)$$

For $\mathcal{V} = 1/6$

$$\frac{A}{a^3} = -\frac{T}{8\mu_1}\frac{(6 - 5\mathcal{V})(1 - 1\,1/2\,K)}{(7 - 5\mathcal{V})} - \frac{T}{8\mu_1}(1 - 2K)$$

$$= -\frac{T}{8\mu_1}\frac{(13 - 10\mathcal{V})}{(7 - 5\mathcal{V})} - \frac{T}{8\mu_1}\frac{(23 - 17\,1/2\,\mathcal{V})K}{(7 - 5\mathcal{V})}$$

$$\approx -\frac{T}{4\mu_1}\left\{ 1 - 1\,1/2\,K \right\}$$

$$\frac{B}{a^5} = \frac{T(1 - 2K)}{8\mu_1(7 - 5\mathcal{V})}$$

$$\frac{C}{a^3} = \frac{T(1 - 2\mathcal{V})}{8\mu_1(7 - 5\mathcal{V})}\left(1 - 2K \right)$$

Putting $K = O$ in these expressions gives the values for A, B and C for the stresses around a spherical cavity ($\mu_2 = O$) and agree with the expressions given by Goodier[7].

It can be seen from the equations for A, B and C that the dependence of the stresses on K (for $K << 1$) depends somewhat on Poisson's ratio, but in no case does the factor which gives the relative change in stress for small K exceed 1-2K. Therefore, in the system under study ($K \approx 0.02$), the stresses around a spherical particle of the low E material differs by no more than 4 percent from the stresses around a spherical cavity. From this it can be concluded that the dispersed low E material for all practical purposes can be regarded as spherical porosity.

THE CARBORUNDUM COMPANY, Niagara Falls, N.Y.
FACTORS AFFECTING THERMAL SHOCK RESISTANCE OF POLYPHASE CERAMIC BODIES, by P. T. B. Shaffer, D. P. H. Hasselman and A. Z. Chaberski, February 1961. 62p. incl. illus. tables and 21 refs. (Project 7350; Task 7350) (WADD TR 60-749, Pt I) (Contract AF 33(616)-6806)
Unclassified report

An investigation of the factors which effect the thermal shock resistance of polyphase ceramic systems has been conducted using the model system zirconium carbide-graphite. The research has been divided into two areas:

(over)

1. Theoretical calculations of the individual material properties, which show that the included graphite particles may be regarded as spherical pores.

2. Experimental data, which substantiate the postulate that increased thermal shock resistance is a result of an increase in the ratio of strength over Young's modulus, brought about by the addition of the low Young's modulus phase .